A review on the modeling of fission chambers

by

Zoairia Lyric

B.S., University of Dhaka, 2006
M.S., University of Dhaka, 2008

A REPORT

submitted in partial fulfillment of the requirements for the degree

MASTER OF SCIENCE

Department of Mechanical and Nuclear Engineering
College of Engineering

KANSAS STATE UNIVERSITY
Manhattan, Kansas

2017

Approved by:

Major Professor
Douglas McGregor

Copyright

Abstract

Fission chambers are ideal neutron flux surveillance instruments to ensure nuclear reactor control and safety. They can provide online, in-core, real-time measurements covering the dynamic range of neutron flux including pulse, Campbell, and current mode over decades of reactor operation cycles. The first patented fission chamber was developed by Baer et al. in 1957. It was a cylindrical assembly thermal fission counter having sensitivity of 0.7 count/neutron cm^{-2} for a background measurement of 5 counts/second with ability to operate at a temperature range of 20-80 ºC [3]. Since then, fission chamber technology was developed to come up with miniature and sub-miniature dimensions withstanding high irradiation and high temperature environment making them suitable for in-core online diagnosis. Since the introduction of high temperature fission chamber technology starting in the 1970's, the need of the advancement in modeling of the fission chambers to improve their performance has become important. The development of modeling depends upon the understanding and consideration of underlying physics of these detectors. The validation of modeling of fission chambers will need the quantification of uncertainty introduced at every stage from neutron-deposit interaction to signal shaping. Based on this objective, a detailed review was performed on fission chamber modeling and simulation covering neutron flux self-shielding, fissile deposit evolution, fission product emission, auto-absorption, electron-ion pair creation, charge recombination and avalanche, space charge effect, charge transport, propagation of electronic pulse and pulse shaping. The analytical methods, algorithmic treatments, simulation, and computation codes used so far in case of modeling different aspects of fission chambers were reviewed. Along with the numerical methods and computer codes for simulating electron drift and charge transport for the usual gas chamber detectors, the use of several fissile material evolution techniques and computation codes were observed in case of fission chamber

modeling. The use higher order statistics to handle fluctuation mode and to treat noisy data were observed. In recent years, fission chamber modeling made reasonable improvement in detail physics modeling. Several analytical methods like advanced statistics for Campbellng mode and electric field distortion due to space charge effect need to be incorporated in computation codes. More progress in the areas of evolution of gas behavior, consideration of Penning, recombination, and avalanche effect still needed.

Table of Contents

List of Figures

List of Tables

Chapter 1

Introduction

Fission chambers are playing a vital role in case of flux monitoring in commercial nuclear power reactors, material testing reactors, mock-up reactors, and in advanced reactor concepts. Several features of fission chambers make them the most suitable in-core neutron monitoring instruments. The development of variety of miniature and sub-miniature versions ensure their in-core adoption without significant reactor core perturbance. Fission chambers offer the freedom to use suitable fissile deposits in their appropriate isotopic composition and thickness to surveil a specific neutron flux (thermal or fast) component.

A single chamber can be used in all three operational modes, i.e., pulse counting, Campbelling or Mean-Square Voltage (MSV) or fluctuation, and current mode. Thus, it is possible to use these chambers to track neutrons from start-up to full power of the reactor. The possibility of overlapping between the pulse counting and the Campbelling mode of a fission chamber enables it to monitor flux over a wide dynamic range [17].

The effective utilization of a fission chamber for a specific reactor depends on the combination of exact modeling and simulation and experimental validation. Fission chamber modeling encompasses single use or coupling among mathematical formulae, algorithms and techniques, generalized or problem dependent computer codes. A number of researchers, e.g., DuBridge [16], Lux et al. [43], Pontes et al. [52], Chabod et al. [13, 14, 15], Poujade et al. [54] provided mathematical modeling for fission chamber operational modes, saturation current, voltage extensions, saturation current considering electric field distortion due to space charge effect, etc. Different algorithms like Kalman filter [61], filtered Poisson process [17] were utilized

in case of modeling the signal of fission chambers. It was observed that drift chamber or Monte Carlo based codes, e.g., GARFIELD [67], MAGBOLTZ [5, 69], heavily used for generic gas-based detector modeling, were also often used for fission chamber modeling. Several researches on fission chamber modeling were done utilizing Monte Carlo Neutral Particle code (MCNP) and Stopping and Range of Ions in Matter (SRIM) code. Several computation codes devoted only to fission chamber modeling, e.g., Fission Chamber Design (FCD) code and CHESTER were developed. Codes like DARWIN, EVO77, ACtivation ABacus (ACAB) code were utilized for deposit evolution and actinide incineration and transmutation calculation.

Development of simulation and computation of fission chambers asks for the consideration of all physical phenomena within the fission chambers from neutron-fissile deposit interaction to electronic signal generation: neutron flux self-shielding, fissile deposit evolution, fission product emission and self-absorption, gas behavior under irradiation, electron-ion pair creation, charge recombination and avalanche, charge transport, electric field screening and electronic pulse shape, and propagation of electronic pulse through electronics [33]. The study at hand reviews the research and development of modeling of fission chambers with special attention given to the treatment of physical phenomena in case of modeling. Chapter 2 reviews the basic physical processes and working principle of typical fission chambers. Chapter 3 describes the evolution of fission chamber technology by describing manufacturing and modeling aspects. Chapter 4 describes mathematical methods, algorithms, and computation codes and their utilization in fission chamber modeling. Chapter 5 illustrates consideration and treatment of different physical phenomena for modeling of fission chambers.

Chapter 2

Principles and Physical Processes of a Fission chamber

2.1 Generic fission chambers

A generic fission chamber is composed of two coaxial electrodes where at least one electrode, generally the inner electrode (anode) is coated with fissile or fertile materials from a few micrograms to a few grams in order to detect neutrons. The chamber is generally filled with a pressurized inert gas at few atmospheres, typically argon at 1.5 bar [33]. Inert gases like argon are used in fission chambers as fill gas to minimize secondary ionization and parasitic contributions. The fill gas pressure is kept nearly equal to atmospheric pressure to avoid gas escaping out of the chamber. The inter-electrode gap can be from tens of microns to a few millimeters. When neutrons interact with the fissile deposit, the nuclei of deposit atoms likely undergo fission with the generation of two heavily charged ions, fission products emission in two almost opposite directions [17, 33]. One product stops either in the fissile layer or in the chamber wall, the other exits from the deposit and ionize the fill gas along its trajectory and creates electron-ion pairs [17, 33, 65]. Provided a DC voltage of a few hundred volts is applied between the anode and the cathode, the electrons and ions drifts across the gas in two opposite directions and thus generate a current signal. The range of the DC voltage should be high enough to collect all the charges, and low enough to avoid the secondary ionization [33]. If these conditions are met, the fission chamber can act like an ionization chamber operating in the saturation regime. The signal of the fission chamber, i.e., the counting rate is then proportional to the fission rate which, in turn, is proportional to the neutron flux. Thus, the signal becomes dependent only on the chamber characteristics and the ambient flux and almost insensitive to the applied voltage [17, 33, 65]. The gamma photons that directly ionize

the filling gas also generate a signal [17, 33]. Gamma signal suppression is one of the biggest concerns in case of modeling of fission chambers.

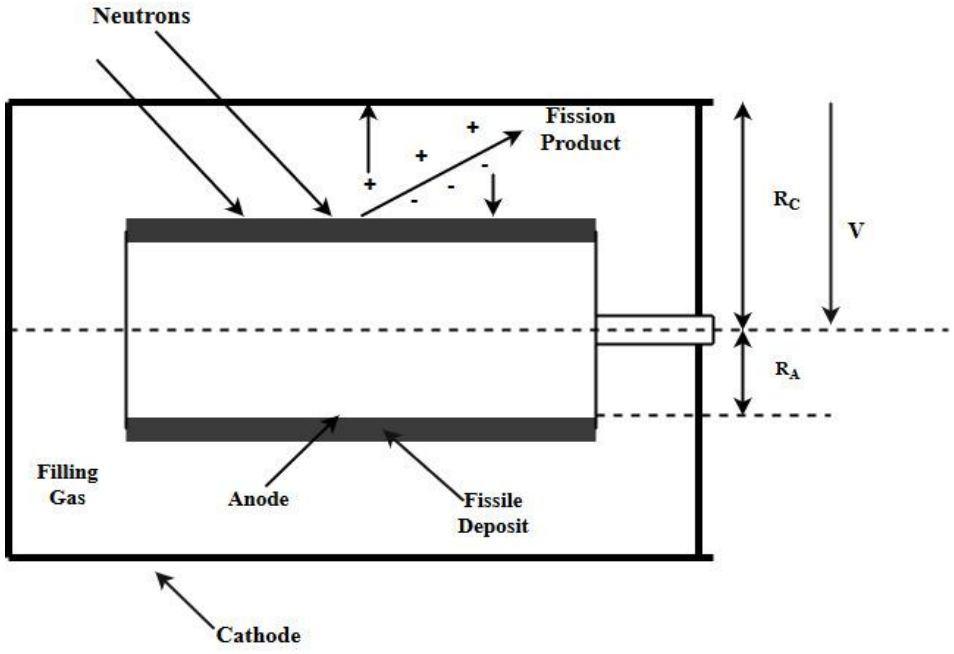

Fig 2.1. Main components and basic operation of a fission chamber, adopted from Jammes et al. [33]

2.2 Three modes of operation

A great advantage of fission chambers in case of being used as in-core instrument is it facilitates the tracking of flux amplitude over a large dynamic range corresponding to about 15 decades of reactor operation. A fission chamber can be operated in three different modes, i.e., (i) pulse, (ii) Campbelling or Mean Square Voltage (MSV) or fluctuation, and (iii) current. These three modes constitute a wide dynamic range depending on the neutron flux magnitude of the system and on the fission rate of the fissile material of the chamber [34].

At ambient low neutron fluxes, the fission rate is so low that each electronic pulse induced by a nuclear fission can be counted event by event [14, 15]. The event rate, being closely related to the fission rate, produces a signal which is a series of well separated pulses to trigger a counter

[25, 34]. The fission chamber can then be operated in “pulse mode” [14, 15, 25, 34]. Monitoring a quantity proportional to the flux is much easier in pulse mode as the average delay between two pulses is much larger than the pulse duration [25, 34]. It is just about finding an optimum discriminator level to eliminate the background noise in the current pulse while measuring the counting rate [24].

As the neutron flux increases, the fission rate becomes sufficiently large so that pulses inside the chamber overlap and can no longer be separated or processed event by event [24, 26]. When the fission rate is greater than a few 10^5 per second, the overlapping of pulses produce a continuous fluctuating signal [33]. The event pile-up generated by the high fission rate calls for a current mode acquisition and the characteristics of the overall current needs to be measured in this case [15, 24]. According to the Campbell theorem, if the basic neutron detection process is Poissonian, the moments of this type of stochastic process depend on the event rate [31]. In other words, the fission rate in this case is proportional to the first two statistical moments of current, i.e., average and variance [24, 26, 33]. So, the “current mode” corresponds to the measurement of average current and the “Campbelling mode" corresponds to the current variance [24].

Current mode poses a challenge to neutron detection because it comes with significant gamma contribution (usually 1- 10% of the signal depending on the geometry) and allows no straightforward way for gamma discrimination. This mode is based on the first part of Campbell's theorem which states the average value of the current from a random current pulse source is proportional to the average pulse rate and thus charge produced per event is proportional to the pulse height. To keep track of gammas in current mode sometimes a simultaneous irradiation of a deposit-less chamber is utilized [69]. The Campbelling mode, representing the second moment or cumulant (variance), offers a much better discrimination against the gammas [33]. The Campbell

mode signal or the variance of the current is proportional to the average pulse rate and to the square of the charge produced per event which in turn is related to the square of the pulse height. The average number of charge pairs created by a single fission product is much larger than that produced by a single gamma ray. Thus, the measurement of the variance of the detector current suppresses effectively the contribution of the low-amplitude gamma-induced pulses if a suitable bandwidth is chosen [69]. The Campbelling mode is of much interest not only for noise reduction from the signal, but also for signal processing over a wide measurement range of 10 – 15 decades and taking advantage of higher order statistics to extract additional information on the detection process quality [25].

2.3 Saturation regime and operating voltage

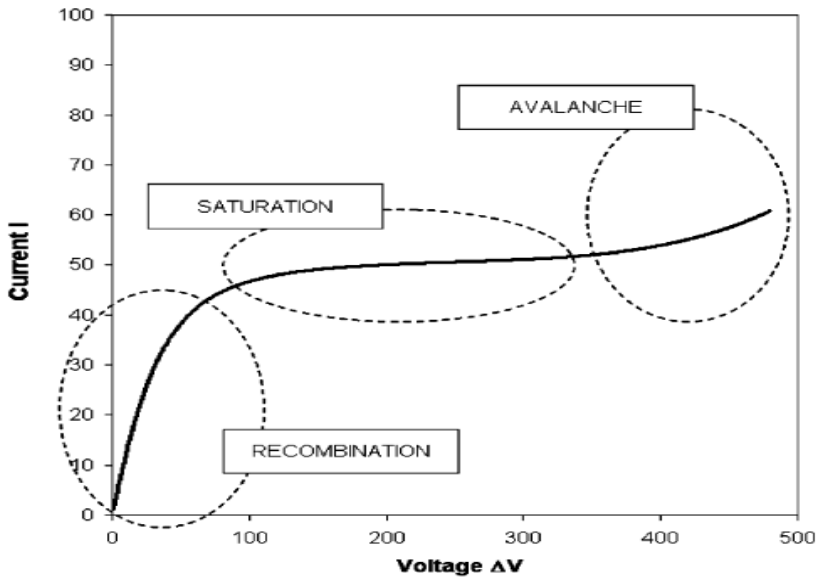

Fig 2.2: The three regions: recombination, saturation, and avalanche in the calibration curve from Chabod et al. [14]

During the current mode acquisition of a fission chamber, the monitoring of the current as a function of bias applied at the electrodes yields a calibration curve consists of three zones: i) recombination, ii) saturation, and iii) avalanche. The saturation regime of this curve demonstrates a plateau where the detector response does not vary with the applied voltage. The output current within this plateau is only proportional to the ambient neutron flux, which is why this curve is referred as the characteristic curve of a fission chamber [14, 15].

Mathematically, for a fission chamber operating within a moderate to high neutron flux environment, the output current of the chamber can be written as:

$$I = \iiint_V (N - kn_e n_a + \alpha(E) n_e v_e) dV \quad (2.1)\ [14]$$

where, V is the inter-electrode gap volume, n_e and n_a are electron and ion densities, E is the electric field in between cathode and anode, N is the density of the charge pairs created by the fission products in the filling gas per unit time on their trajectory, v_e is the average drift speed of the electrons in the filling gas, k is the volumetric recombination co-efficient and α is the Townsend's first ionization coefficient which can be interpreted as the probability of impact (secondary) ionization by an electron per unit differential path length of travel [45]. The $kn_e n_a$ part represents charge loss due to electron-ion volumetric recombination, the $\alpha n_e v_e$ term arises from the secondary ionization by high speed electrons. [14]

Thus, the current, I in (2.1) is the combination of three contributions:

$$I = I_{REC} + I_{SAT} + I_{SEC},$$

where,

$$I_{REC} = -e \iiint_V kn_e n_a dV$$

$$I_{SAT} = -e \iiint_V N(\underline{r}) dV$$

$$I_{SEC} = e \iiint_{V} \alpha(E) n_e v_e \, dV$$

(2.2) [14]

I_{SAT} in (2.2) represents the constant current zone or the current delivered within the saturation plateau. This current depends solely on the detector's intrinsic characteristics and the ambient neutron flux. The plateau is adjusted on the left by the contribution of the current due to recombination, I_{REC} and on the right by that of the current due to secondary ionization, I_{SEC}. Thus, the saturation regime acts as the reference for the voltage limits within which a fission chamber in a high flux environment should be operated [14, 15].

Chapter 3

Evolution of fission chamber technology over time

The progress in fission chamber modeling requires an understanding of the evolution of fission chamber technology over time. The basic concept of fission chambers originated in the 1940's during the Manhattan Project [35, 57]. Although the concept developed at that time was far from what could be applied for in-core instrumentation, the fundamental *principles* of fission chambers have not changed much. By reviewing the literature on fission chambers from the original to the contemporary work it was determined significant changes in the *technology* can be subdivided into each decade. Based on this review, it is evident that France was and still is the pioneer in this technology in every aspect with other contributors from UK, USA, and some from Japan.

1940 - 1950:

Different designs of fission chambers, e.g., parallel-plate, flat, multiple-plate, spiral, were investigated. The parallel-plate type designs which yielded high counting rate contained up to 750 mg of U_3O_8 (63% enriched in U-235) on each plate. These plate type designs were operated with a voltage between 100 – 200 volts at pressures of 1.7 -3.4 bar of argon [57].

1951-1960:

During this decade, the fission chamber technology became mature enough to be used in reactor control. Baer et al. at Westinghouse Electric Corporation in the early 50's started working on a high sensitivity "fission counter" able to operate when exposed to neutron fluence as high as 4×10^{15} neutrons/cm^{-2} [1, 2, 3]. In 1952, Baer et al. explored how the change in sensitivity was related to the change in inter-electrode gap or the fissile deposit (U-235) thickness in the case of fission counters. The coating thickness of 2.0 mgcm^{-2} and an electrode gap of 0.381 cm were found

optimum to achieve an increase in sensitivity by varying the discriminator setting of the linear amplifier [1]. In 1957, the continued investigation led Baer-Bayard-Swift to come up with a patented technology of a tri-uranium octoxide (U_3O_8) coated, permanently sealed off, cylindrical assembly thermal fission counter capable of enduring severe operational conditions such as temperature up to 80◦C and gamma radiation of 1 kGy/h at maximum. The sensitivity of the counter was 0.7 counts/neutrons/cm^2 with the discriminator set for an alpha background counting rate of 5 counts/second [1, 2, 3, 35]. The goals for their effort went beyond achieving high sensitivity to thermal flux and minimum response to noise. The objectives also included operating in a wide range of temperature (up to 80 °C), withstanding severe shock and vibration, providing a novel structure for electric discharge [3]. At the same time, the first-ever "fission chamber" to measure a flux of slow neutrons with the minimum measurable flux of the order of a few thermal neutrons/cm^2/s was patented in France [34, 38]. This device could operate in an intense gamma environment and exhibited excellent temperature resistance [38].

1961-1970:

In the early 60's, Guéry [30] came up with the patented specification of a miniature neutron-fission ionization chamber suitable for utilizing in power reactors as it was able to operate without much flux disturbance even for high flux gradients and could be used at temperatures up to 300 ºC. It was claimed that the chamber could be used in homogeneous reactors where corrosion phenomena were serious. The two electrodes and other pieces of the proposed chamber were made of less neutron-absorbent material like Zr or Zr alloy. The internal electrode was deposited with fissile material. This work done at Commissariat a l'Energie Atomique et aux Energies Alternatives (CEA), France was dedicated specially to experimental nuclear reactors [30, 35].

From the in-core instrumentation need of fission chambers, the high temperature fission chamber (HTFC) technology got developed starting from the late 60's. The earliest HTFC documentation was from U.K. by Goodings in 1969 [27, 28]. One article from Goodings [27] described a series of radiation detectors developed within the 60's. Among them there were pulse counting (chambers that can be operated in pulse mode, lower flux levels) and DC (chambers that can be operated in direct current mode, higher flux levels) fission chambers which were the first kinds to withstand temperature as high as 500◦C or higher for in-core use in challenging environments like gas-cooled or sodium-cooled power reactors for a maximum three-year period. In parallel, several smaller fission chambers (6 mm or 3 mm external dia-) which were either pulse counting chambers for use in heated zero reactors or mean current chambers for flux scanning or irradiation experiments in Materials Testing Reactors were developed. Huge improvement in the quality of mineral insulated cables also came along with these versions [27]. Another article from Goodings presented theoretical and experimental findings on the physical parameters responsible for parasitic residual currents of the DC fission chambers [28].

1971-1980:

In France, the first HTFC of 10-mm diameter was developed to be operated at the maximum temperature of 450◦C for the absolute measurement in the experimental fast reactor RAPSODIE in the early 1970's. Within this period, the endeavor was focused mainly on initial experimental need and preliminary design. Thorough studies were done on the selection and treatment of the materials. Additionally, the importance to clean and outgas all the fission chamber components at the operational temperature under a secondary vacuum was pointed out. The active volume of the detector (chamber with electrodes and fill gas) was kept separated from the seal assembly (connection with mineral-insulated cables) to keep the temperature homogeneous [34]. The idea

of using a quenching gas like CH_4 or N_2 with the fill gas to minimize the charge collection time was suggested. However, the problem of possible gas decomposition under irradiation or gas combination with the other materials of the fission chamber was also predicted. It was also suggested to reduce the high voltage bias from 200 V down to a few 10 V in order to prevent breakdown pulses from occurring in the mineral insulant [34].

In the 1970's, a major development program for the French fast breeder reactors was conducted and managed by the French Atomic Energy Commission (CEA) in close collaboration with their industrial partner, what was then Philips Electronics, and is now PHOTONIS. A European collaboration between France, UK, and Germany was also maintained until the early 1990s. The program aimed to develop, manufacture, and qualify a new family of HTFCs and associated electronics covering a wide dynamic range. In the surveillance and control in the extremes of temperature and gamma irradiation of the fast breeder reactors, HTFC's ability was investigated in two essential functions: in-vessel integrated neutronic control and clad failure detection by integrated detectors. Three main types of detectors CFUE, CFUD, and CFUC which varied mainly in sensitivity ($10^0 – 10^{-2}$ cps/ncm^{-2}s^{-1}) or in dimensions (7-48 mm diameters) were tested by placing either inside the thimble (250℃) or in the core region (600℃). CFUE types had less sensitivity and dimension as they were tested in the core region tested for a thermal-equivalent fluence of 10^{19} ncm^{-2} [34, 53, 63].

In 1974, Popper et al. reviewed the ongoing developments of neutron instrumentation for fast reactors in France, Germany, United Kingdom and United States. Studies in the United States were reported on the use of the Campbelling mode to avoid the gamma contribution from the signal. The successful performance of the HTFCs in the Experimental Breeder Reactor (EBR-II) at 385 ◦C in the flux of 10^{10} ncm^{-2}s^{-1} and the gamma dose of 10kGy/h for several thousands of

irradiation hours were reported. It was also reported UKAEA (UK Atomic Energy Authority) recommended not to use nitrogen as quenching due to the nitriding effect [53].

In 1976, Hasegawa et al. of University of Tokyo proposed a novel neutron flux measurement system for fission chambers to achieve wide range measurement by utilizing the linear relation produced by the pile-up of pulses between the neutron flux and the threshold voltage of an amplitude discriminator on log-log scale [31].

1981-1990:

The development of HTFC in U.K. [27, 28, 53] paved the way to utilize the technology in the unique case of decommissioning experiments of the Windscale advanced gas-cooled reactor in the early 80's [29]. Nine sets of fission chambers were utilized in neutron monitoring for a wide range of experimental high power and temperature transients [9, 29].

From the late 80's to the early 90's, investigation on HTFC's capability to operate on wide-range of measurements (pulse counting, mean-square voltage, direct current) started. CFUC07 type HTFC was developed to operate over a wide range for roughly 10 decades, from start-up to full power. For CFUC07, preliminary tests on the operation at high temperature, irradiation endurance tests under a gamma irradiator and the neutron sensitivity and wide-range capability in the ULYSSE thermal experimental reactor were performed. Several experiments were done involving the CFUC07 keeping it in the same in-vessel position till January, 2010. [34, 63].

1991-2000:

As HTFC's were utilized in commercial power plants, the need to house six to seven fission chambers in fixed coaxial positions in light water reactors (LWRs) rose in the late 90's. Bignan et al. in 1994 patented sub-miniature fission chamber design of 1.5 mm diameter containing 200 mg of fissile material with a tight feedthrough between the fission chamber body and the coaxial wire.

This design was due to an effort to bridge the technological gap from the mobile 3 mm chamber in LWR's to the fixed multiple coaxial in-core instrumentation. The major change of sub-miniature fission chambers (SMFC's) over the miniature fission-chambers (MFC's) was not only in their smaller dimensions (1.5 mm dia), but also in the utilization of a special nickel and alumina gas-tight feedthrough between the chamber body and the mineral cable to maintain the fill on the level of the sensitive part [6, 8].

By the end of the last century, a group of CEA researchers (Lescop et al., Trama et al.) worked on a project named MARINE (French acronym for automated neutron measurement), under CEA and their industrial partner Technicatome, which involved upgrading the existing analogue monitoring system and developing a fully digitized wide-range neutron surveillance system covering all 10 to 11 decades of operation [40, 62]. They utilized a CFUL08 type ex-core fission chamber to produce wide dynamic range of signals for Marine project [40].

2001-2010:

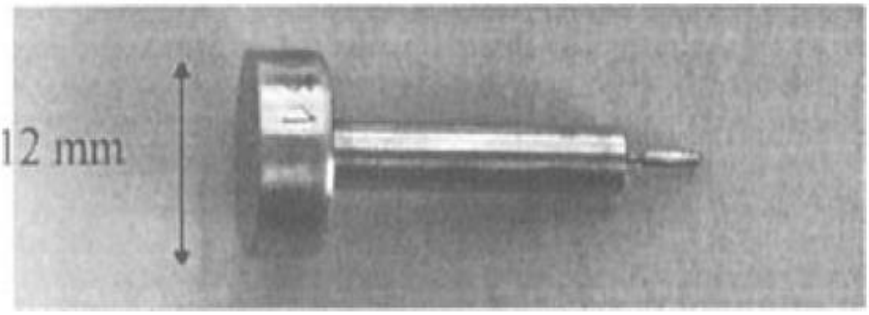

Figure 3.1: Plate type fission chamber with diameter of 12 mm from Blandin et al. [7]

In 2001, Blandin et al. documented the endeavor carried out by The Reactor Measurement Systems Laboratory (LSMR) of the CEA/Cadarache on designing, modeling, manufacturing, and development of several miniature fission chambers which vary in type (cylindrical or plate), in diameters (1.5, 4, or 8 mm) nature of fissile deposit (uranium or other actinides), the mass of the

fissile deposit, and the nature (argon, helium) and pressure of the fill gas. Figure 3.1 shows a 12 mm diameter plate type fission chamber with inflexible extension piece.

Development of in-house computer codes to predict current-voltage characteristics (FCD3) and fissile deposit evolution (EVO77) was in important part of this study [7]. Future transmutation studies using two types of deposit (U-235 and another actinide) in the same chamber body was also mentioned and this idea was put into effect on 2002 for fission micro-chambers (1.5 mm diameter) under the Mini-Inca project [7, 19].

In 2002 and 2003, a thorough research work on subminiature fission chambers for their neutron sensitivity, gamma effect, current-voltage characteristics, long term behavior up to 2.10^{21} ncm^{-2} in the current mode was done utilizing both the modeling with FCD code and experiments in the research reactor BR2 (Belgian Reactor 2) under Nuclear Measurement Systems Laboratory (LSMN) of CEA/Cadarache [8, 68].

In the next two years, the documentations regarding the extension of MARINE project, IRINA (French acronym for automated in-core neutron instrumentation) which introduced a novel wide range in-core neutron monitoring system to measure the thermal flux in the range of 10^7 - 10^{14} $ncm^{-2}s^{-1}$ and at 300º C were available. Along with the manufacturing of a new miniature detector (3 mm dia) able to work in the aforementioned flux range and temperature, this endeavor basically involved designing a complete electronics system to accompany the detector operation in all the three operating modes - pulse, Campbelling, and current continuously by the extensive use of digital technology and advanced digital signal processing [41].

In 2005, Oriol et al. published their work on several sets of initial experiments on the first prototypes of the industrial versions of the CEA sub-miniature fission chambers (in-pile CFUZ-53) under high thermal neutron fluxes (up to 4.10^{14} $n/(cm^2.s)$) in the CALLISTO loop of the BR2

reactor in PWR-like conditions. They presented an analysis of the results for neutron sensitivity, linearity to thermal neutron flux, current/voltage characteristics, gamma contribution, temperature effects and long term behavior and compared the experimental data with calculation results from a fission chamber theoretical model [49].

In 2004 and 2005, Ohmes et al. and McGregor et al. of Semiconductor Materials and Radiological Technologies (S.M.A.R.T.) Laboratory of Kansas State University, USA published their effort in developing a novel miniaturized parallel plate type fission chamber named "Micro-Pocket Fission Detectors (MPFD's)" for real-time, near-core, and in-core flux monitoring. The basic design of this type of detectors is a neutron reactive coating enclosed in a gas pocket size as small as 0.5 mm wide with a diameter of 1 mm [44, 47].

Chabod, et al. in 2006, came up with a theoretical model to predict and analyze the operation of fission chambers in current mode in high neutron flux environment considering a lot of physical processes occurs in the current mode [13]. Filliatre et al. in 2008 and 2009, under the Fast Neutron Detector System (FNDS) project of the Laboratoire Commun d'Instrumentation CEA–SCK**.**CEN (LCI), showed why Pu-242 is the most suitable fissile deposit for the on-line fast neutron flux monitoring in a high neutron flux environment utilizing reference CEA computation code, DARWIN for fissile deposit evolution [20, 22].

In 2006, Ohmes et al. published the performance characteristics of MPFD's in terms of neutron reaction energy deposition, background sensitivity, detector speed, detector lifetime. A prototype of 3 mm diameter electrode was tested in the neutron beam port of KSU TRIGA Mark II reactor [48].

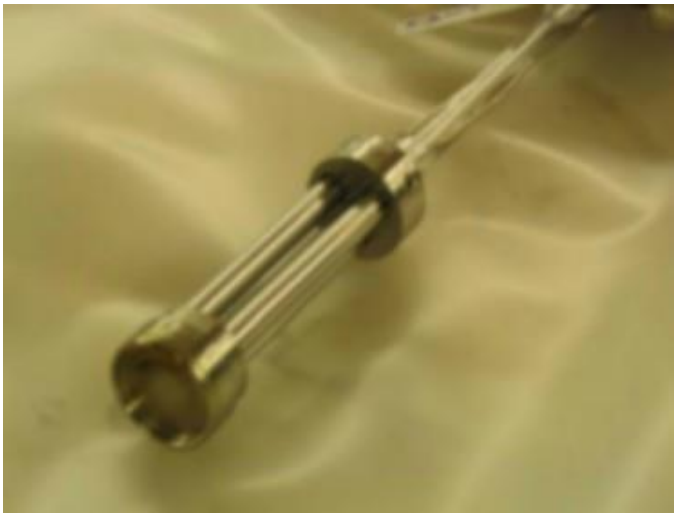

Figure 3.2: Triple deposit fission chamber from Letourneau et al. [42]

In 2009, Chabod et al. presented mathematical modeling to calculate saturation current and to extend the voltage domain of the saturation plateau of the miniaturized fission chambers [14, 15]. In the same year, Filliatre et al. introduced an algorithm to estimate the thermal and fast flux simultaneously at discreet times for a mixed spectrum and thus proposed a way for the joint operation of a fast fission chamber and a thermal monitor. The basic idea of the algorithm was to form linear system of equations to express the signal of the detector by considering the superposition of thermal, epithermal, and flux component of the flux and solve the equations in matrix form to get the eigenvalue (detector signal) [21]. In the same year, Geslot et al. presented the work done in Dosimetry Command Control and Instrumentation Laboratory (LDCI) at CEA/Cadarache on development, design, and manufacturing of miniature and subminiature cylindrical fission chambers (1.5 – 8 mm dia) for in-core or near-core flux measurement for fissile deposits other than U-235 [24]. In 2009, Letourneau et al. presented experimental campaign done to test the miniature chamber performance in current mode under the neutron flux up to 10^{14} $ncm^{-2}s^{-1}$ and the temperature up to 400◦C in severe irradiation environments like high flux reactors or

powerful spallation neutron source. The factors limiting the distortion of electric field were discussed and a novel idea of "back-to-back" triple deposit fission chamber (TDFC) to follow the burnup of minor actinides for transmutation studies were proposed. This TDFC is composed of three electrically independent, 4 mm diameter fission chambers which are mechanically connected and sharing the same gas (Figure 3.2). Two chambers have different deposits (U-235 and another actinide) and the third chamber is devoid of deposits. In this way actinide fission current with respect to the current due to U-235 standard fission can be measured. The third chamber can help in measuring parasitic currents [42]. Vermeeren et al. showed how the dominance of gamma signal when measuring fast flux through fission chambers can be suppressed by operating the chambers in Campbell mode [69].

In 2010, Jammes et al. published their effort to model the signal delivered by a fission chamber using DARWIN and GARFIELD code suit [33].

2011- Present:

In 2011, Jammes et al. evaluated the high temperature fission chamber technology (HTFC) to be utilized in French Fast Reactor Program by discussing the operational conditions in sodium-cooled fast reactors, the HTFC technologies investigated and developed in France and worldwide and the French HTFC technology in the light of "technical readiness levels" (TRL) concept [34]. In 2012, Filliatre et al. presented a way of computation based on the open source GARFIELD code suit for the neutron induced charge spectrum and pulse shape for fission chambers [23]. In the same year, Jammes et al. paper investigated how the fissile coating aspects affect uranium fission chamber signal sensitivity combining a Monte Carlo simulation results and experimental data [35]. In 2014, Geslot et al. explored the impact of fill gas mixture and pressure on chamber sensitivity in Campbelling mode by comparing the results for both pulse and Campbell modes. Experiments

were done in the low power Minerve reactor of CEA/Cadarahe using the in-house refillable 8 mm miniature chamber CF8R [25]. In 2015, Elter et al. presented the results of inquiries into the linearity of the pulse and Campbelling mode, crucial for the feasibility of the wide-rage operation of a fission chamber, by developing a Poisson pulse train simulation code which simulates the pulse trains of a fission chamber and thus does a quantitative analysis of the mode linearity [17].

The research on advanced versions of MPFD's were published by Unruh et al., and Reichenberger et al. in the recent years. [56, 66]. Development and validation of contemporary MPFD's at nuclear reactor test facilities, e.g., Transient Reactor Test Facility (TREAT) were reported in 2013 [66]. Advancements in electrodeposition technique, measurements of neutron reactive material, numerical optimization, detailed MCNP simulated performance for MPFDs were documented in 2014, 2016, and 2017 [55, 56, 51]

Chapter 4

Modeling of Fission Chambers

4.1 Mathematical methods

Chabod et al. developed a theoretical model to predict and analyze the characteristic response of fission chambers in current model [13]. The evolution of the calibration curves was analyzed as a function of different physical parameters such as gas pressure, gas composition, applied voltage, fission rates, inter-electrode gap, anode radius during various conditions of irradiations. The model predicted that the Xenon contamination in the fill gas during irradiation could affect the saturation plateau drastically (the avalanche would happen at a lower voltage in consequence). It was also observed that if the reduction of the inter-electrode gap can lessen the perturbations associated with high fission rates, e.g., space charge perturbation, curve deformation, the diminishing of the plateau [13].

Chabod, S. in another work presented detailed mathematical formulae for the saturation currents for the four main geometrical configurations, namely, circular plane, rectangular plane, cylindrical, and spherical miniaturized fission chambers operating in current modes and thus provided a reasonable way to calibrate the in-core chambers [14].

Chabod, S. and Letourneau, A. presented a theoretical model to predict the voltage extension of the saturation plateau as a function of fission chamber physical characteristics like geometry and fill gas properties by solving a system of three nonlinear differential equations relating to charge conservation and Maxwell-Gauss formula. The results from the theoretical treatment showed that at high neutron fluxes the saturation domain could vanish if chamber characteristics like fill gas properties and chamber geometry are not optimized. Results also

showed rare gases like krypton and xenon exhibit better performance than argon to maximize the voltage range for saturation plateau. To improve the accuracy of the calculations, data for the electron-ion recombination coefficient for rare gases at successive pressure intervals within the whole range is needed [15].

DuBridge described the system concepts, design, and results of utilizing Campbell's theorem for neutron detection for both in-core and out-of-core applications. The Campbell signal (the variance of a current) which is proportional to the average pulse rate and the square of the pulse height, produces a better discrimination against the background radiation induced measurements [16].

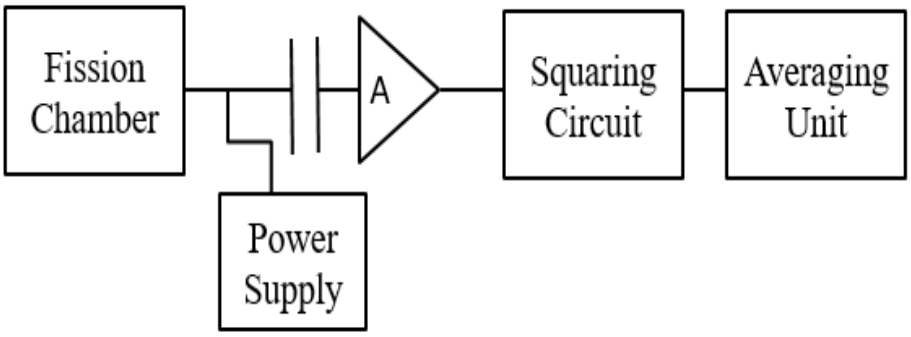

Figure 4.1: A functional block diagram for a Campbell system, adopted from DuBridge [16]

A simplified Campbell system consists of a detector or sensor, power supply, amplification unit, squaring circuit, and averaging unit. If the detector generates pulses randomly, the instantaneous value of a signal, I can be subtracted from the average value, $(< I >)$, this subtraction can be amplified by an alternating current (ac) amplifier. It is possible to square and average this amplified signal using squaring and averaging units so that the output signal is the variance of the original signal from the detector:

$$< I^2 > - < I >^2 = (I - < I >)^2 \qquad 4.1 \text{ [16]}$$

The quadratic dependence of the detector signal on the neutron flux provides a basis for measuring noise over a wide range. DuBridge suggested in [16] that use of higher moment about the average value of the current would lead to better gamma discrimination. This suggestion was the motivation for Lux et al. [43] in providing detailed mathematical treatment for higher order Campbell techniques. The assumption of the method provided by Lux et al. is if the detector response is a random variable, the average can be derived in mean current technique, variance in Campbell technique, and some combination of its moments up to n in the n-th order Campbell technique [43].

More theoretical work on higher order Campbell technique was performed by the publication of Pontes et al. [52]. This research utilized the generalization of Campbell's theorem to calculate the n-th order spectra of the current signal of a detector. A numerical model was developed to demonstrate the method for an ionization chamber. The proposed theorem, in the form of nth-order spectra, with the shape of current pulses represented by a vector of random parameters, allowed a more detailed, higher order statistical characterization of radiation detectors than the existing second order treatment [52].

The approach of using n-th order moments and spectra formula described in [52] was used by Geslot et al. in their experiment to calibrate fission chambers in Campbelling mode [25]. In this research, they characterized detector pulses and calculated detector response using a detailed expression of Campbell's second theorem. The fission chamber response was characterized based on fission rates. In this way, the detector calibration coefficient was independent of the neutron spectrum and could be determined prior to the experiment. Thus, this method avoided a major drawback of empirical calibration in Campbell mode in which calibration measurements must be done in a similar environment where the detectors would be utilized [25].

4.2 Algorithms and Techniques

4.2.1 Extended Kalman Filter (EKF) Algorithm:

For digital signal processing, extended Kalman Filter (EKF) algorithm is often used for optimized prediction. It was used in MARINE wide range neutron monitoring system to generate flux and reactor period information [61]. If the following exponential equation which represents the relationship between flux, time, and period as the base equation:

$$\varphi(t) = \varphi_0 e^{\frac{t}{\tau(t)}} \quad 4.2\ [61]$$

where, φ represents neutron flux in $ncm^{-2}s^{-1}$, t is the time in seconds and $\tau(t)$ is the period in seconds.

The digitized version of this equation can be treated as state equation:

$$\varphi_{k+1} = \varphi_k e^k \quad 4.3\ [61]$$

This equation can be interpreted as the relationship between fluxes at time k and time $k + 1$

The expansion of the digitized version of this flux model:

$$\varphi_{k+1} = \varphi_k(1 + k + 0.\frac{k^2}{2} + \cdots) \quad 4.4\ [61]$$

The two-dimensional state vector can be written as:

$$x_k = \begin{cases} \varphi_k \\ k \end{cases} \quad 4.5\ [61]$$

The noise-less, ideal observation or measurement is:

$$z_k = x_k \quad 4.6\ [61]$$

But, in real case, there will be noise in both state or process and in the observation.

$$x_{k+1} = \varphi_k(x_k) + w_k$$

$$z_k = x_k + v_k$$

4.7 [61]

where, w_k is the noise associated with state and v_k is the noise associated with observation.

It is not possible to exactly determine the observation noise. But, according to EKF, the optimum prediction of the state can be possible by considering both the observation and previous estimated state.

$$\hat{x}_{k+1} = \hat{x}_k + g_k(z_k - \hat{x}_k)$$ 4.8 [61, 77]

where, $\hat{x}_k$ and $\hat{x}_{k+1}$ are the estimated states at time k and $k+1$, g_k is that induce optimization [61, 77].

4.2.2 Filtered Poisson Process:

The mathematical model behind considering the fission chamber signal as a Poisson pulse train is known as filtered Poisson process. It is a stochastic process where the time interval between two successive events has exponential distribution with an intensity parameter [17]. In case of fission chambers, this intensity parameter is proportional to the ambient neutron flux level, i. e., to the fission rate. The successive events are pulses. Hence, the output is the superposition of pulses and can be expressed by:

$$\varphi(x, t) = x.f(t)$$ 4.9 [17]

Equation 4.2 represents the form of the pulses where $f(t)$ is the constant shape function normalized to unity and multiplied by x, the amplitude of a random pulse. Every single pulse has an arrival time, t_k according to an exponential distribution and an amplitude x_k. The fission chamber signal can be described as a Poisson pulse train defined by the following equation:

$$n(t) = \sum_{k=0}^{N(t)} x_k f(t - t_k)$$ 4.10 [17]

The upper limit of the summation, $N(t)$ is the random variable of the Poisson distribution, i.e., cumulative number of counts in the detector.

4.2.3 Algorithm for joint estimation of the thermal and fast components:

The neutron spectrum is assumed to be composed of three components: thermal, epithermal, fast. The thermal component can be described by Maxwell distribution, the epithermal component can be described by $1/E$ slope within a piecewise function with thermal and fast limit values, and the fast component can be described by the Watt expression. The joint estimation algorithm tries to estimate the thermal and fast components, φ_1 and φ_2 respectively at discrete times t_k. If there are two detectors, detector a and b to monitor thermal and fast components respectively, the signal of the detector can be expressed in the matrix form:

$$\begin{pmatrix} S_a(t_k) \\ S_b(t_k) \end{pmatrix} = M \begin{pmatrix} \varphi_1(t_k) \\ \varphi_2(t_k) \end{pmatrix} \quad \text{4.11 [21]}$$

The sensitivities to the two detectors to each component of the spectrum are different enough and so the matrix M can be inverted to give the estimations [21].

4.3 Simulation and Computation Codes:

The development in fission chamber modeling came up with the development of several computation codes, DARWIN, EVO77, ORIGEN-S, and ACtivation Abacus (ACAB) code for fissile deposit evolution. These codes differ mainly in two ways: i) how they solve the differential equation to find new isotopic composition, ii) the types of nuclides they deal with. SRIM (Stopping and Range of Ions in Matter) was used in chamber modeling to simulate the fission product trajectory (to find range and straggling of products and to find stopping power). The use of computation codes for generic gas based detectors like GARFIELD and MAGBOLTZ was observed in case of fission chamber modeling. MAGBOLTZ was used mainly to compute electron drift. In some research works, GARFIELD was used to simulate signals by making interface with

both MAGBOLTZ and SRIM and accepting input from these two codes. Some codes like fission chamber design (FCD), CHESTER were developed exclusively to compute the physical characteristics of small size fission chambers. Monte Carlo N-Particle (MCNP) code was used to produce fission rates or flux perturbation factors.

4.3.1 DARWIN

DARWIN is a code system developed at French Atomic Energy Commission (CEA) to compute deposit evolution [64]. This code was written in FORTRAN with some C functions and can be run on different operating systems like Unix, Linux, or Windows. This code is capable to deal with almost all types of radionuclides like fission, activation, and spallation products and actinides and its application covers nuclear fuel cycle, dismantling, radiation detection, shielding, thermonuclear fusion, accelerator driven system, nuclear medicine, etc. The DARWIN package is a combination of data libraries (DARWIN libraries), two code interface programs (PSAPHY and INTERPREP), and the depletion unit program PEPIN2. The DARWIN libraries are based on basic nuclear data like cross section and decay data. The decay data and cross-section libraries of the depletion module, PEPIN2 are basically from but not limited to JEF2 [38], ENDF/B6 [18, 74], EAF97 [59]. The neutronic data (self-shielded cross-sections and neutron fluxes) are provided by the French transport codes like TRIPOLI, APOLLO2, and ERANOS. The main program PEPIN2 solves the generalized coupled differential depletion equations (Bateman equations) to give the result as the concentration of each isotope versus irradiation or cooling times. The evolution of a specific isotope can be tracked by a search engine in this package and several physical quantities like isotope mass, concentration, activity, radiotoxicity, alpha, beta, gamma spectra, neutron production by spontaneous fission or (alpha, n) reaction, residual heating for any cooling times can be calculated [64].

4.3.2 EVO77

EVO77 is an evolution computer code developed by Hervé Recroix of The Reactor Measurement Systems laboratory (LSMR) of the CEA/Cadarache to keep track of the isotopic evolution of the fissile deposit. This code considers 77 heavy nuclei and hence the name is EVO 77. For any initial isotope, EVO77 solves the classic differential evolution equation utilizing Runge-Kutta algorithm [7].

4.3.3 ORIGEN-S:

ORIGEN-S, based on the ORIGEN [74] code developed at Oak-Ridge national laboratory, is a SCALE [75] system module to compute the time-dependent concentrations of nuclides subject to depletion, decay, and transmutation [32]. ORIGEN-S retains the same matrix exponential method to solve the ordinary differential equations of ORIGEN [32].

4.3.4 ACtivation ABacus (ACAB) Code

This code was developed to perform activation and transmutation calculations by space-dependent inventory calculations, treating decay transitions considering every nuclear reaction, treating actinides and fission products, simulating realistic operational scenarios [58]. The basic computation method (way of solving differential equation) of ACAB is the same as ORIGEN code (matrix exponential expansion model). The impact of activation cross-section uncertainties on activation related quantities can be investigated by ACAB uncertainty calculations. There are mainly two types of error propagation techniques used in computational simulation to find the systematic propagation of uncertainty: i) adjoint/forward sensitivity analysis procedures and ii) Monte Carlo technique [11]. ACAB calculates uncertainty by Monte Carlo method [11, 58]. The application of Monte Carlo methodology for uncertainty analysis requires information on the joint probability distribution of the nuclear data errors [11].

4.3.5 SRIM

SRIM, a set of computer programs to calculate the Stopping and Range of Ions in Matter, was introduced by J.F. Ziegler and J.P. Biersack in the early 80's. Since then it has become a heavily used program over several areas of science and engineering, and major upgrades are offered approximately every six years. With the latest upgrade, an improved correction is available for the stopping of ions in compounds. The latest version of SRIM has a module which allows SRIM stopping and range values to be controlled and read by other programs. Interatomic potentials for all ion/atom collisions are included in SRIM [70].

The SRIM code was utilized for modeling of fission chambers in case of simulating the trajectory of fission products using the stopping power (energy loss per unit length), the range and straggling calculation. Thus, SRIM helped in developing reliable evolution model for fissile deposits. One example of straggling calculation by SRIM found in [14] is provided below:

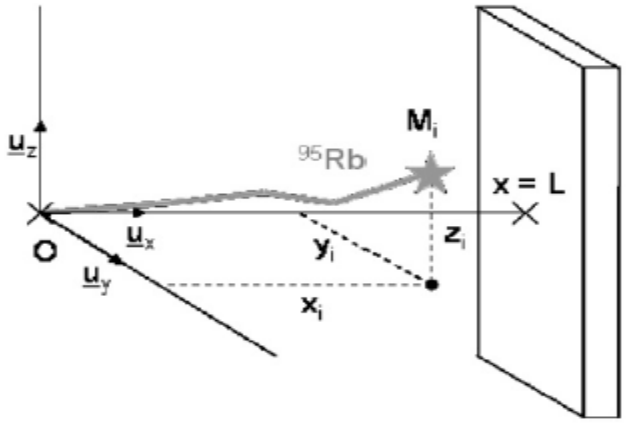

Figure 4.2: Schematic fission product trajectory during a SRIM simulation from Chabod et al. [14]. The fission product is Rb-95 in this case.

Let us consider a fission product, I, which is emitted from the origin (0,0,0) towards a screen placed at a distance L where the space between $y0z$ plane and the screen is filled with a

known gas (Figure 4.2). The random collisions of the fission product with the gas atoms deviates it from its straight-line trajectory along u_x. If the end point of the product is $M_i$with coordinates $(x = x_i < L, y = y_i,\ z = z_i)$ between the $y0z$ plane and the screen, the lateral deviation or straggling, σ_i of the fission product, L is the deviation of the end point M_i compared to the straight-line trajectory [13]. Mathematically from Figure 4.2,

$$\sigma_i = \frac{\sqrt{y_i^2 + z_i^2}}{x_i} \qquad 4.12\ [14]$$

4.3.6 GARFIELD

GARFIELD is an open source two- and three-dimensional drift chamber simulation program developed in CERN. GARFIELD simulates the behavior of drift-chambers by calculating and plotting the electrostatic field, the electron and ion drift, currents of the sense wires produced by the charged particle trajectory through the chamber. The program was primarily written for two-dimensional drift chambers or multiwire counters made only of thin wires and infinite equipotential planes in which case most of the times exact fields are known. The recent developments in GARFIELD made it deal with increasingly popular but hard to analyze detectors containing dielectric media or complex electrode shapes. GARFIELD's ability to accept 2D and 3D field maps computed by finite element programs like Ansys, Maxwell and such enables GARFIELD to handle complex problems where analytic techniques fail. The other recent improvements in the GARFIELD code is enhanced cluster generation and improved signal calculation [67].

4.3.7 MAGBOLTZ

MAGBOLTZ, written by Dr. Biagi from the university of Liverpool, is a Monte Carlo based gas simulation program to determine the drift velocity of an ionization electron inside a gas chamber type detector. The drift velocity is calculated by the integration of Boltzman transport

function. Every MAGBOLTZ input should be modified depending on the gas mixture, the pressure and temperature of the detector and the field information of the co-ordinate point of interest [5, 72]

4.3.8 Fission Chamber Design (FCD) code:

As the flux increases, the rate of charge pair creation also increases. The drift velocity of the electrons and ions (mainly) is not high enough to catch up with the charge collection time. The pile up of charges create space charge phenomenon. Provided all the physical parameters and the technological features of the chamber are specified. The Fission Chamber Design (FCD) computer code, written for the chambers operating in current mode, is based on a theoretical model that considers the electric field distortion due to space charge effect [7, 8, 54]. FCD calculates the neutron sensitivity and the limits of the fission chamber saturation domain by using the applied voltage and the fission rate of the deposit [7, 8]. The calculated neutron sensitivity is given by the following formula:

$$S_{calc} = \frac{I_{SAT}}{\varphi} = \prod eLI_cP\frac{\mu_s}{M}N_a\sigma_f(r_c{}^2 - r_a{}^2) \qquad 4.13\ [8]$$

where,

S_{calc} = calculated neutron sensitivity (ratio of output current to the ambient flux, unit A/(ncm^{-2}s^{-1}))

I_{SAT} = saturation current

φ = ambient neutron flux

e = charge of the electrons

L = sensitive length

I_c = Number of ion pairs created produced by a fission product per unit length per unit pressure

P = Pressure of argon

μ_s = surfacic mass of the fissile deposit

M = Molar mass

N_a = Avogadro Number

σ_f = Fission cross-section

r_c = radius of the cathode

r_a = radius of the anode

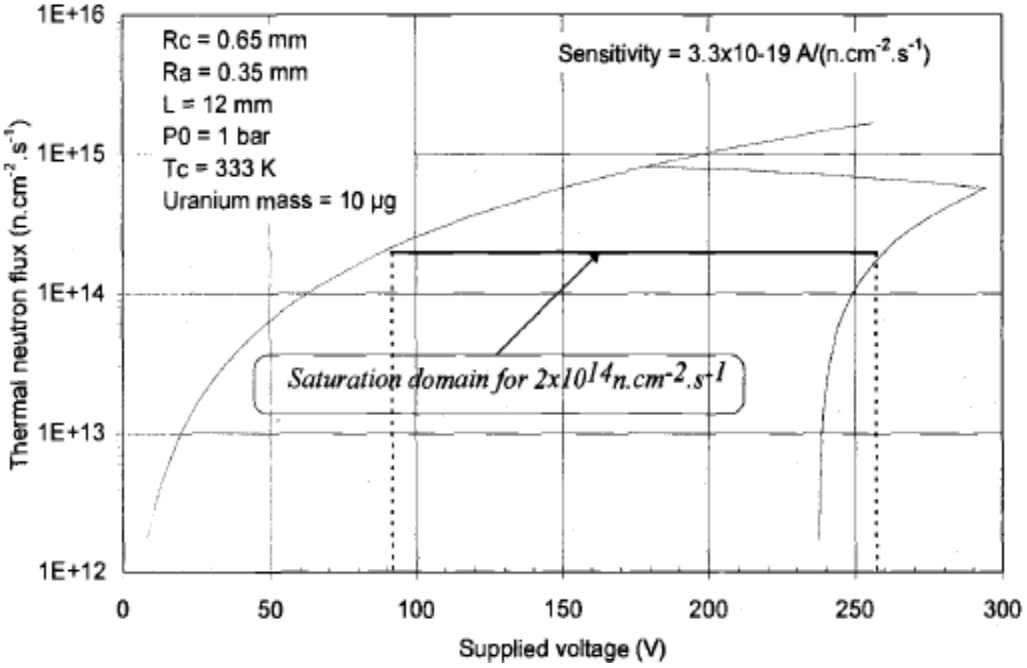

Figure 4.3: Graphic output file generated by FCD code from Blandin et al. [7]

4.3.9 CHESTER:

Based on the GARFIELD suite, CHESTER is a CEA developed Monte Carlo code that aims at simulating the whole physical process of the fission chambers [26]. This code utilizes

SRIM to compute the range of the fission products in filling gases. Recent developments in the code enables it to simulate saturation curves based on the method presented in [14, 15] [26].

4.3.10 Poisson Pulse Train Simulation Code:

Poisson pulse train simulation code, based on the filtered Poisson process, was written in MATLAB to address the question of linearity of the pulse and Campbelling mode. The code takes the pre-defined pulse shape, amplitude distribution, count rate and time resolution as input and produces Poisson pulse train as output. As amplitude and the charge distribution are related, the user can also define the integrated value of the pulse, i.e., the charge of the pulse [17].

The integration of the pulses in case the order of count rate gets comparable to the order of time resolution of the simulated signal makes sure the current delivered by the pulses is not lost. Additional time signals such as background noise or further Poisson trains can be added to the original pulse train. The code has the capability to deal with arbitrary pulse shapes, amplitude distributions, and the added noise. The code suffers from the memory issue as for the requirement of longer measurement time to obtain good statistics will generate large amount of data. The extrapolation of the pulse trains at points where they ended rather than generating a new one at the end point has been adopted to solve the memory issue [17].

4.3.11 Monte Carlo N-particle (MCNP) transport Code:

The general purpose MCNP code was developed and is maintained by Los Alamos National laboratory to calculate mainly the transport of neutral particles (hence, N-Particle), i.e., neutrons, gamma rays, the transport of secondary gamma rays resulting from neutron interactions by Monte Carlo method [60].

4.4 Modeling based on algorithms, computation codes and other techniques:

Biagi, S.F. presented a faster and accurate Monte-Carlo simulation code that can bypass complexities of solving Boltzmann transport equation for electron drift and diffusion computation in gases [5]. The calculations of the drift gas properties done by the existing codes like MAGBOLTZ involves numerical integration of the Boltzmann transport equation. Some breakdowns were observed in the MAGBOLTZ computation in predicting the accuracy due to the improper simulation of the large anisotropy in the velocity of the electrons in the direction of the electric field. The faulty simulation often arises because of not taking higher order terms in the spherical harmonics or Legendre polynomials in the truncation of the energy distribution function. Improved accuracy in calculating drift velocity by 1% was achieved by MAGBOLTZ when it uses an expansion up to the third Legendre polynomials for the solution of the energy distribution function but it also requires unrealistic computation time. To solve this problem, the program presented used Monte Carlo integration technique to solve the transport equation which is fast enough to converge to an accuracy of 0.5% in only about 10 seconds. The generic solution offers the flexibility of arbitrary angles in between magnetic and electric field. The cross-section data base for gases in MAGBOLTZ can be used with this program [5].

The computation program presented here can help optimize any gas radiation detector design including the fission chamber being used in large magnetic fields. The computation methods can help simulate exact electron transport within the detector interface [5].

Blandin et. al in their research under Reactor Measurement Systems laboratory (LSMR) of the CEA/Cadarache on in-core fission chambers utilized a calculation chain based on computer codes like MCNP, FCD, EVO77 (Figure 4.4) [7].

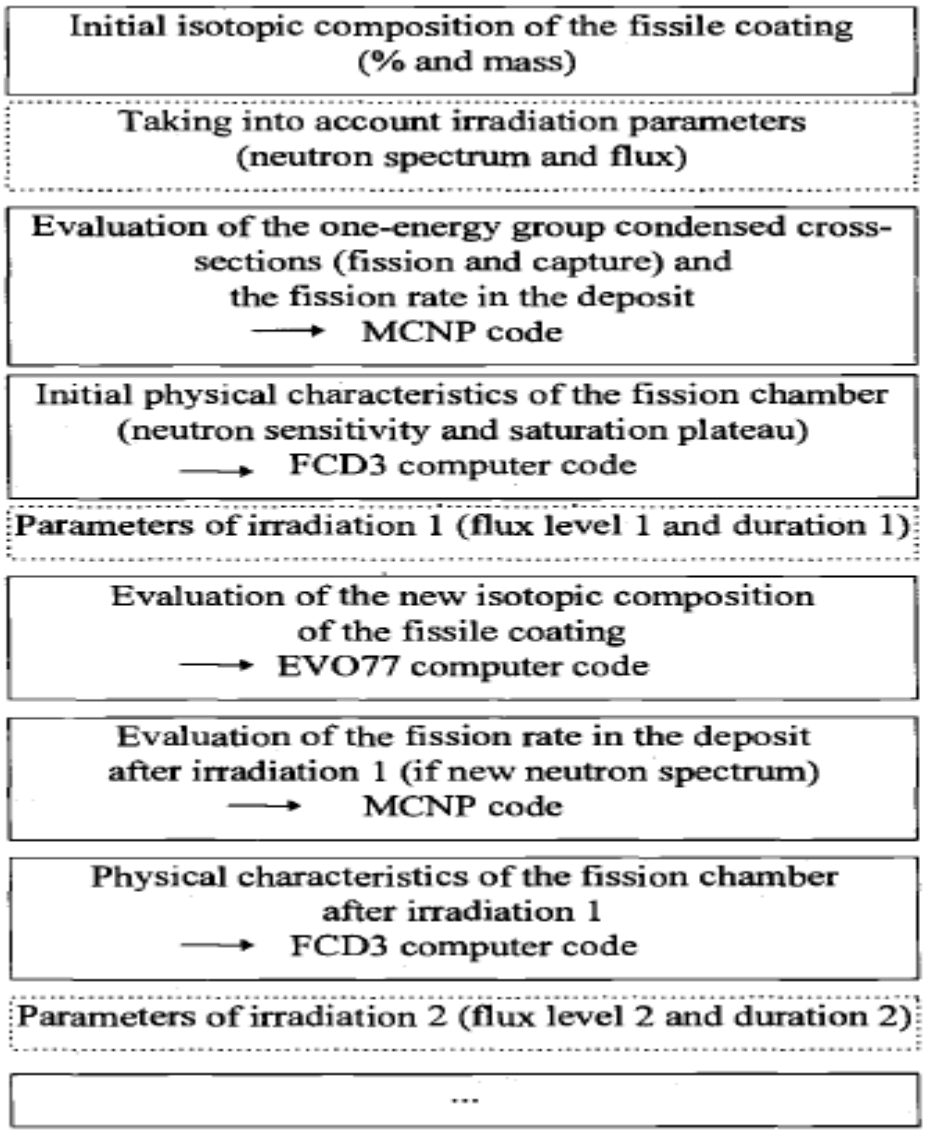

Figure 4.4: General calculation chain for fission chamber design developed by Blandin et al. [7]

The chambers developed for in-core use varied in their type, e.g., cylindrical or plate, in diameters, e.g., 1.5, 4, or 8 mm, nature of fissile deposit, e.g. uranium or other actinides, the mass of the fissile deposit, and the type and pressure of the fill gas. The physical characteristics of the detectors, e.g., geometry, fissile material coating, gas pressure get adjusted according to the type of the neutron spectrum and flux environment they would be put into and the set of the neutronic

parameters, e.g., spectrum indicators, fission rates, integral neutron cross-sections, they were supposed to measure [7].

The need to predict the chamber current-voltage characteristics and deposit evolution for each specific chamber made LSMR develop a calculation chain involving three codes, two in-house ones, FCD (works only for current mode) and EVO77, and MCNP. MCNP takes into account the isotopic composition of the fissile deposit, the irradiations and evaluates the 1-group condensed cross-sections and fission rate. FCD takes the MCNP evaluated parameters as input and gives initial physical characteristics of the fission chamber (neutron sensitivity and saturation plateau) as output. Based on the evaluated cross-sections and fission chamber characteristics, the isotopic evolution will be calculated by EVO77. The MCNP then again does the evaluation of the fission rate after one irradiation and then FCD takes input and the cycle goes on. The predicted results with this chain matched nicely with the experimental ones for two miniature models CFUR43 and CFUF43 of external diameters of 3 and 4 mm respectively. The possibility of further validation of FCD code for sub-miniature fission chamber saturation characteristics and neutron sensitivity prediction for transmutation studies were mentioned by Blandin et al [7].

The use of FCD code was also found in the research of the development of sub-miniature fission chambers (SMFCs) in terms of modeling and experiments in current mode under CEA/Cadarache's Nuclear Measurement Systems Laboratory (LSMN) [8]. Three sets of SMFC's were prepared to carry out the experiments – two with fissile deposit (SMFC3, SMFC4), the third one (SMFC2) identical to SMFC4 but with no fissile coating. The coating-less chamber was used to keep track of the noisy current resulted from two sources – current induced in the cable due to the radiation-induced drop in the cable insulation resistance and current mainly due to gamma in the ionization chamber zone. The first current was the function of the cable length and the second

one depended on the intensity of the radiation field perceived in the sensitive zone. The current-voltage characteristics remained constant for long term performance and sensitivity loss was a function of consumption of fissile content. The FCD code prediction of the lower limit of saturation domain matched with that in the experimental curves. An agreement in the order of neutron sensitivity in FCD prediction and experimental results was observed but the undershoot in the magnitude by the code indicated the theoretical model was much too simplified and needed refinements [8].

For the research on developing mathematical formulae of the saturation current for the predominant geometrical configurations of the fission chambers in current mode Chabod et al. utilized SRIM [14]. The steps were to develop general formulae to evaluate charge pair density in the inter-electrode space and then to evaluate saturation current and then to apply and to modify these formulae for different chamber configurations by making necessary approximations. The constant law hypothesis (fission products would travel in straight lines in miniaturized detectors) was adopted in this case. Hence, the quantification of the impact of the constant law hypothesis of the straight-line trajectory of the fission products for several millimeters and constant atmospheric pressure and perturbations in saturation current in case of diversion from this law were needed. SRIM helped in this case to check the lateral deviation or straggling, σ of the fission products (Rb-95 in this case) after a collision ranging from 1 to 10 mm for common fill gases like helium, neon, argon, krypton and for varying pressures from 1-5 bars (Figure 4.5). A better statistic was obtained for calculating the average straggling, $\langle\sigma\rangle$, by taking 49,999 histories. The analytical distribution of straggling values, σ_i using equation 4.4 was calculated. It was confirmed the constant law hypothesis for small sized chambers held for trajectories of several millimeters and P ≈ 1 bar [14]. SRIM was utilized also to plot the evaluation of the kinetic energy of fission products according

to the distance covered by the fission products in the inter-electrode space for four inert gases mentioned earlier.

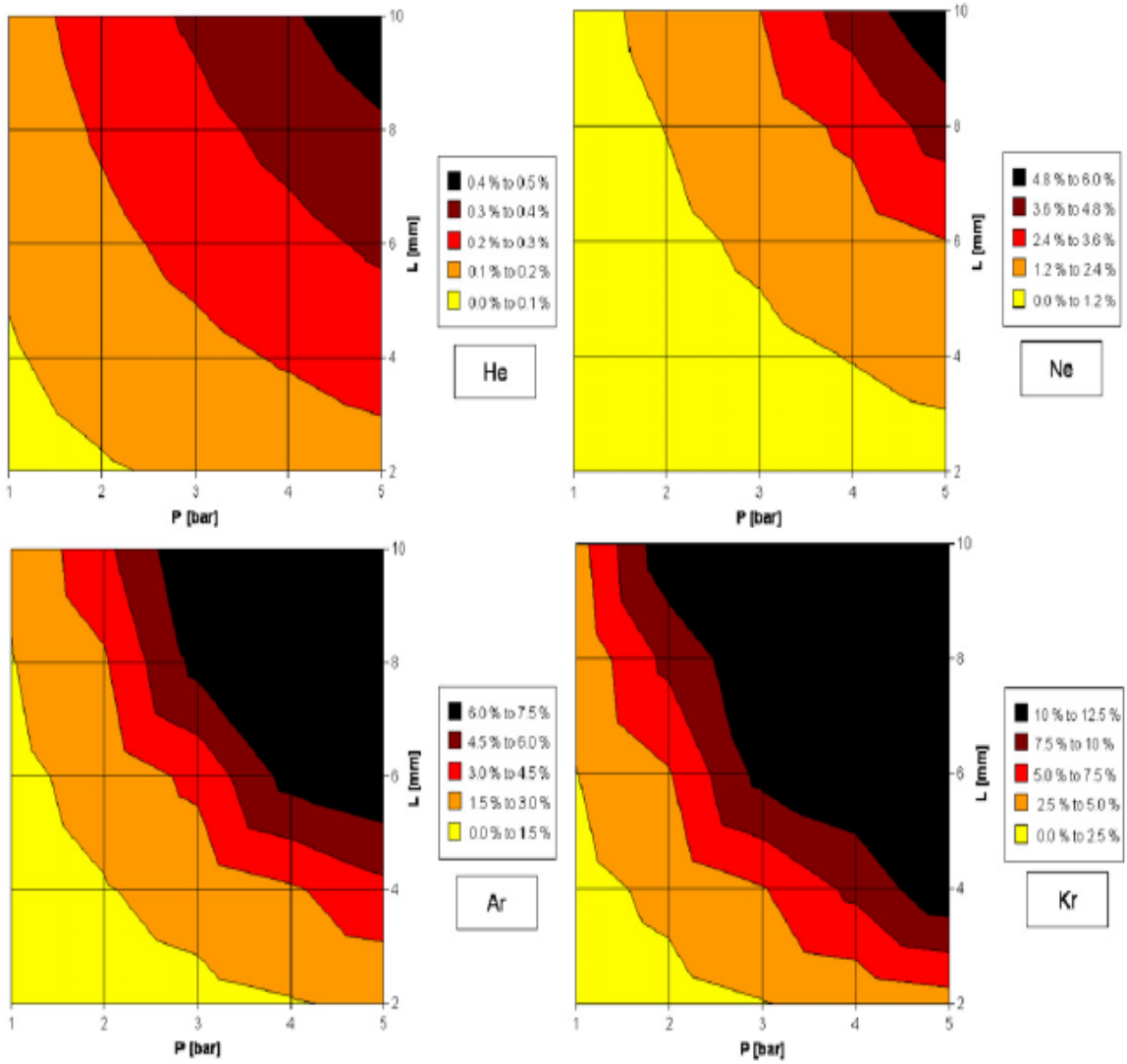

Figure 4.5: SRIM simulation of average straggling, $\langle\sigma\rangle$ for Rb-95 fission products according to pressure, p and distance, L for inert gases, He, Ne, Ar, Kr, from Chabod et al. [14]

The use of MCNP and evolution code CINDER was reported by Fadil et al. in their research to use fission micro-chambers for transmutation studies in high intensity neutron flux environment [19]. A single deposit fission chamber (SDFC) with U-235 fissile coating was used for the qualification and the measurement of flux intensity with a motive to use the knowledge to develop

an innovative double deposit fission chamber(DDFC) containing U-235 and another actinide in current mode to transmute the minor actinides. The deposit evolution was simulated using CINDER code and it was proposed to use isotopically purer U-235 deposit to eradicate the uncertainty due to Pu-239 buildup. MCNP code was utilized to compute neutron flux in the experimental channel [19].

The utilization of DARWIN was reported by Filliatre et al. in their research to support Pu-242 as the most suitable fissile deposit for the on-line surveillance of the fast component of flux that coexisted with significant thermal component in a high neutron flux environment [20, 22]. The potential fissile deposit candidates for the fast neutron monitoring were selected maintaining these criteria: (i) it would be used as a single fissile deposit, (ii) would be predominantly sensitive to fast neutrons, (iii) would have a half-life greater than one year, (iv) would not have unsuitable toxicity and volatility. To be in accordance with the second criterion, the inequality, $\bar{\sigma}^{fast} \geq 3.3\bar{\sigma}^{th}$ was chosen because for the experimental system (BR2 – Belgian Reactor 2) spectrum, $\sigma_{th}/\sigma_{fast} = 3.3$ [20, 22]. The MCNP computed spectrum for BR2 reactor is shown in Figure 4.6.

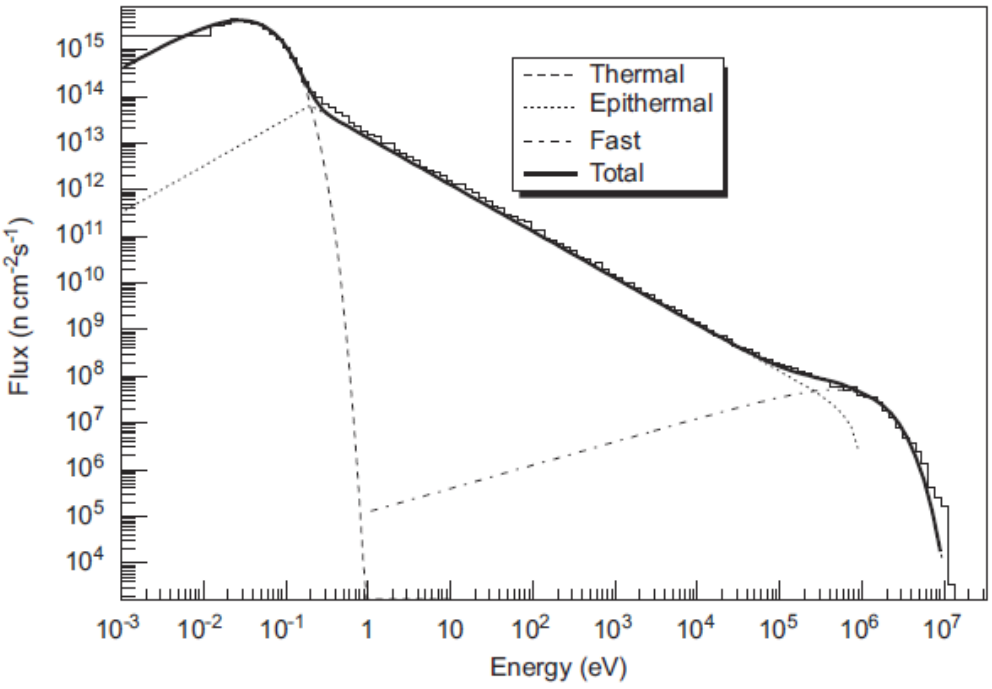

Figure 4.6: MCNP simulation of the spectrum of the K311 channel of BR2 reactor from Filliatre et al. [20]

DARWIN, the reference CEA evolution computer code was used to analyze of sensitivity to fast neutrons, to simulate the evolution of isotopic contents under irradiation in a high flux and to compute the fission rates for all potential isotopes as the best candidate for fast neutron monitoring [20, 22]. It was mentioned earlier in this chapter of the report, DARWIN computes isotopic evolution by solving generalized Bateman equations. The library sets: JEF2.2 [38] and EAF97 [18] used for DARWIN simulation yielded similar results with insignificant differences. The best choice was found as Pu-242 for its high and stable sensitivity to fast neutrons over a wide range of total fluence (up to 10^{21} n/cm^2). The results showed that the sensitivity of Pu-242 to fast neutrons was not only excellent at the beginning of the cycle but also decreased reasonably slowly with fluence. All deposits contain some impurities and so along with the simulations done for pure Pu-242, two isotopic compositions of Pu-242 were checked for the sensitivity to fast neutrons [20,

22]. Because of the considerable thermal fission rates of impurities like Pu-239 and Pu-241, an isotopic composition of Pu-242 that minimizes these two impurities would be a better fissile deposit [20, 22].

In the extension of the previous research, under the Fast Neutron Detector System (FNDS) project of the Laboratoire Commun d'Instrumentation CEA–SCK.CEN (LCI), Filliatre et al. introduced an algorithm that estimated thermal and fast flux simultaneously at discreet times for a mixed spectrum and proposed the co-function of fast and thermal on-line detectors in a high neutron flux environment [21]. Although, fast neutron monitors like Pu-242 are excellent at the beginning of a cycle, they tend to get sensitive to thermal neutrons due to evolution over time. A separate thermal neutron monitor like U-235 or SPND of similar specifications should have to be allied with the fast flux monitor to keep track of the thermal component and the proposed algorithm can help for their joint evaluation. The algorithm considered the equation for the detector signal expression as a two-energy matrix eigenvalue problem (as the two different sensitivities give the characteristics of two types of detectors) and solved it for fast and thermal flux. Here, the user had the privilege to define an energy cut-off, the initial states of the detectors, the shape parameters, the fission rates measurements of the detectors, and cross-section data to compute the deposit evolution. DARWIN with JEF2.2 library data were used to simulate the fission rates. The algorithm was implemented in C++ using an object-oriented data analyst framework "Root" [73], developed by CERN. The sensitivity of the algorithm to the input model accuracy was tested keeping the flux constant to an initial value. It was found that the uncertainty for thermal flux comes from a constant which depends primarily on the detector location. For the sensitivity test where a Gaussian noise was added, a minute increase in the standard deviation of the flux values

was observed. For the last test of variable flux, a delay time of 36 s was taken immediately before and after each change. The flux values remained the same [21].

The algorithm proposed in [21] should be a solid one to use in case of mixed flux monitoring evaluation since the tests sensitivity tests prove the algorithm itself does not introduce any noticeable bias, can handle slightly noisy data and large relative variations of flux components very well. Taking small finer, non-regular temporal meshes considering the expected variation of the flux, reducing measurement error, accuracy of cross-section data, and spectrum model was prescribed for this algorithm [21].

Filliatre et al. presented a simulation route based on the open source GARFIELD code suit for the neutron induced charge spectrum and pulse shape for fission chambers [23]. The MAGBOLTZ code, one which is fully integrated within GARFIELD was used to compute electron drift parameters using a Monte Carlo technique. The SRIM code was utilized alongside to simulate the trajectory of fission products using the stopping power (energy loss per unit length), the range and straggling. For the sake of a good statistics, the electron/ion pairs were generated in a group of clusters within GARFIELD with the advantage of user tuned maximum number of clusters. It was observed larger histories per cluster can make the clustering bias negligible. When several CEA versions of the fission chamber were tested under this computation, it was found that the chambers having smaller inter-electrode gap, could not reflect the whole energy distribution in the charge spectrum (a physical effect). For chambers having larger gap, the charge collection was larger. For the only chamber, which had fissile coated cathode, double peaks were observed within a larger spectrum because a higher percentage of fission products were stopped in the gas. The pulse shapes were triangular for all chambers except for the cathode-coated chamber which had

an inverted pulse shape compared to the others. The ion collection time was found to be three orders of magnitude greater than the electron collection time. The application to current and Campbelling mode showed that both the mean current and spectral density depends on the fission rate. It was found that the spectral density was dependent but mean current is independent of sampling frequency. Thus, not only this computation route provided spectroscopic information or pulse shape but also opened the door to compute mean current and variance [23].

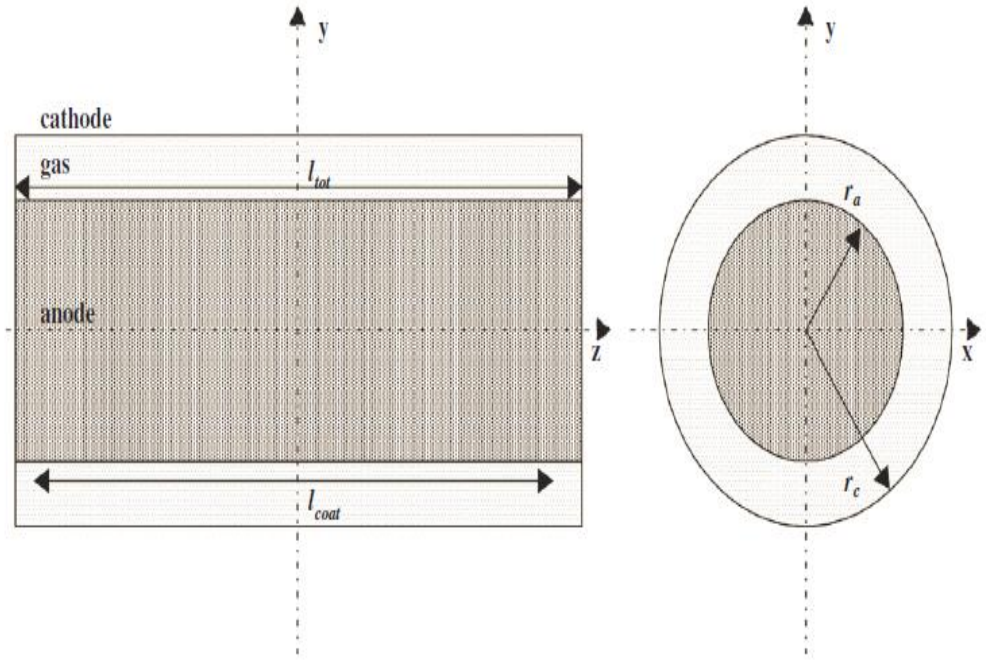

Figure 4.7: Schematics of fission chamber used in simulation route from Filliatre et al. [23]

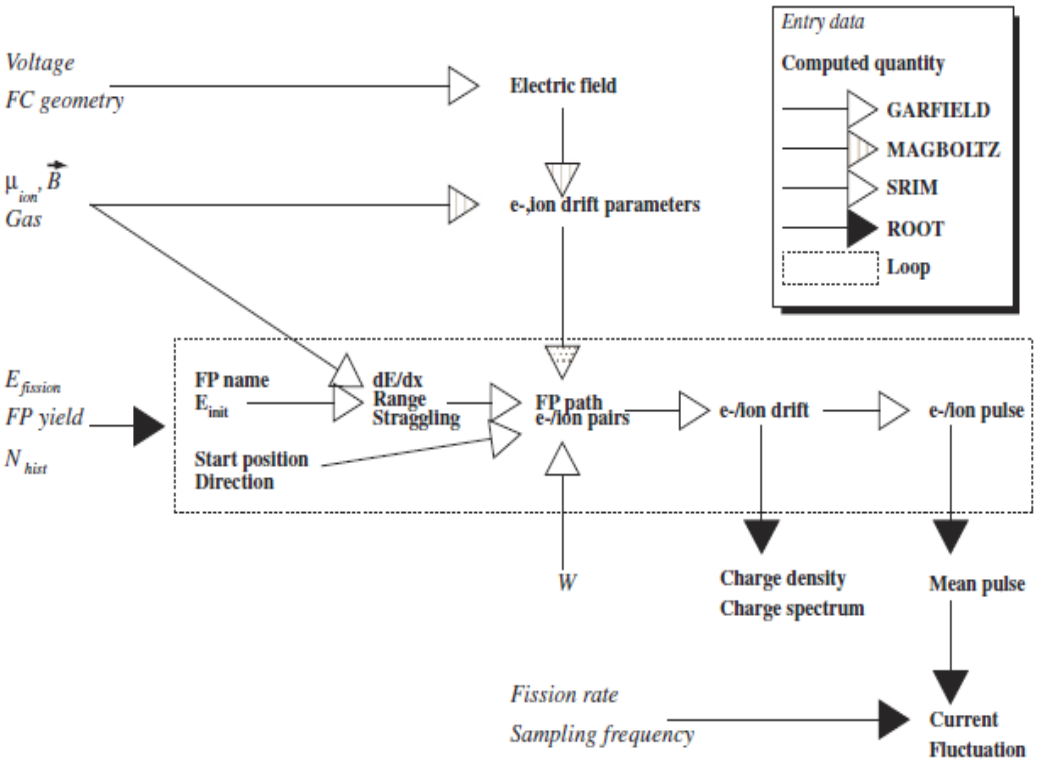

Figure 4.8: Diagram of the simulation route developed by Filliatre et al. [23]

The application of CEA Monte Carlo code, CHESTER was reported by Geslot et al. to find the impact of fill gas mixture and pressure on chamber sensitivity in Campbelling mode by comparing the results for both pulse and Campbell modes [26]. Experiments were done in the low power Minerve reactor of CEA Cadarahe using the in-house refillable 8 mm miniature chamber CF8R. The Campbell mode signals which is proportional to the square of the Mean Fission Product Charge (MFPC), i.e., the square of the mean charge deposited by the fission products, showed the same pattern obtained by pulse mode measurements in exhibiting maximum sensitivity around the gas pressure of 3-4 bars within the 1-9 bar range experimented. The gas mixture types used were pure argon, and argon mixed with quenching gas (argon with 4% N_2 and argon with 10% CH_4 (P10)). The experimentation was yet incomplete because of the use of low 300 V bias, a standard

saturation regime could not be set up. The higher gas pressure raised the recombination process and thus lowered the detector sensitivity. For this reason, an extrapolation technique was used to extrapolate the saturation curves up to 1 kV. The results were verified using CHESTER simulation. It was found that maximum detector sensitivity is independent of the type of the gas mixture owing to the fact that charges were produced mainly for the argon atoms. The extrapolation and simulation results confirmed a saturation region will be achieved starting from 1 kV for 4 bar fill gas pressure. The initiation point of fission rates for Campbell mode for this detector indicated an overlapping range for both pulse and Campbell and showed the possibility of using this device for the whole reactor operation range as a fixed in-core monitor [26].

Jammes et al. in their review on the research activities regarding modeling of the signal delivered by a fission chamber presented the utilization of DARWIN, GARFIELD, MAGBOLTZ, SRIM and SPICE [71] in a number of studies [33]. Each individual study recorded here belonged to one of the three major groups – i. simulation of deposit evolution, ii. The impact of bias voltage and filling gas properties on charge collection time, and iii. Simulation of a pulse signal prior to amplification. The simulation of the deposit evolution was done with DARWIN with the conclusion that Plutonium 242 was the best choice for fissile isotope to monitor the fast component of the neutron flux for a specific fluence (10^{20} - 10^{21} n.cm^{-2}) for MTR (Material Testing Reactor) spectrum. The impact of bias voltage and filling gas properties on the charge collection time was investigated analytically for the positive ions and with the use of computer codes for the electrons, taking drift velocity as a function of reduced electric field in both cases. The fact that the positive ions are subject to Brownian motion paved the way to calculate their transport analytically utilizing the mobility concept when electric field is weak enough to be considered as just the noise in the Langevin equation. The transport of electrons was computed by the MAGBOLTZ code embedded

in GARFIELD. The fission product trajectory using energy loss and straggling was done by SRIM. The fission chamber signal filtering through the pre-amplifier was modeled using the SPICE code. The results showed that the addition of some molecular nitrogen to the argon filling gas and the release of oxygen by the oxide of the irradiated deposit material are both favorable to electron speeding up. The simulation of the electric pulse produced by the fission chamber before amplification for the current and Campbelling mode was done GARFIELD. The results show that the fission chamber signals depend on W-values (the average energy needed to produce an ion pair). The smaller the W-value, the higher the signal amplitude. It suggests that a good knowledge of W-value is essential for the exact simulation of signal amplitudes in current and Campbelling mode [33].

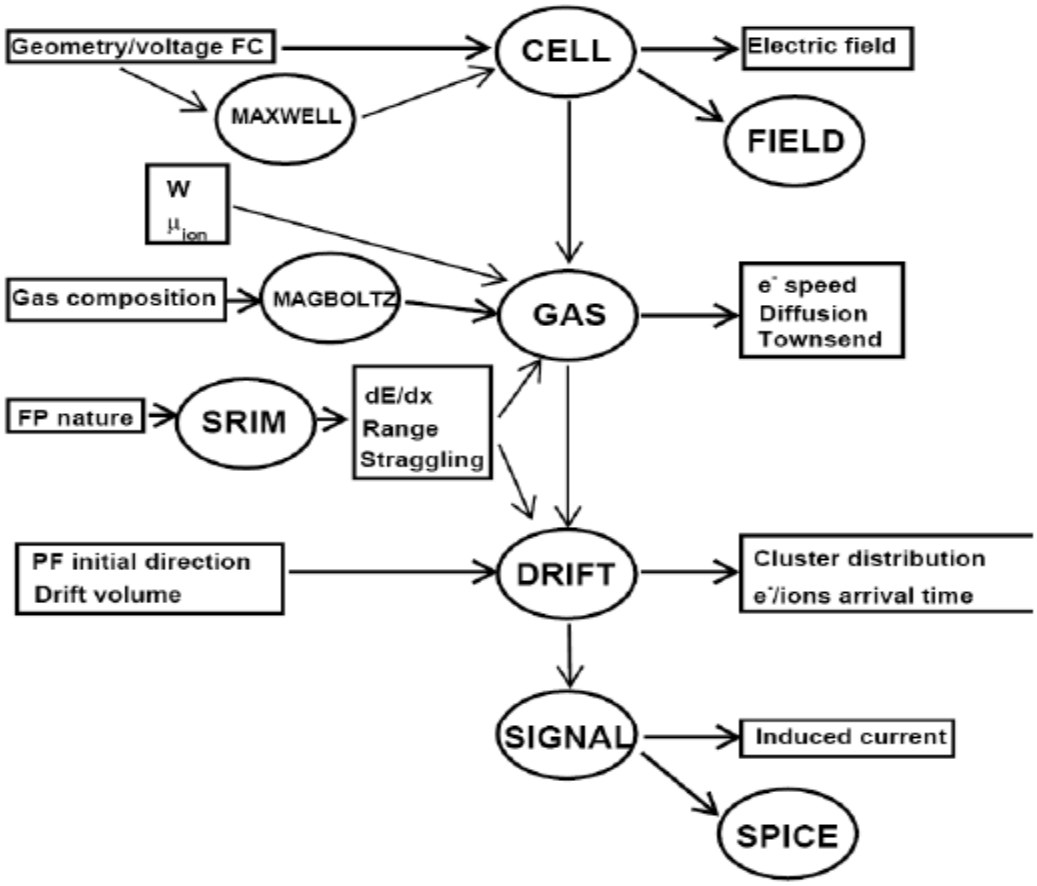

Figure 4.9: Outline of the GARFIELD code suit utilized by Jammes et al. [33]

A Monte Carlo simulation approach was described by Jammes et al. in [35] to investigate how the fissile coating thickness affected uranium fission chamber signal sensitivity. The Monte Carlo program able to handle cylindrical geometry was developed to simulate the distribution of the energy released by fission products in either the fissile coating or in the filling gas. For the simulation, the initial kinetic energy of a randomly chosen fission product in the fissile gas was obtained from both the fission non-relativistic kinematics and the most probable total kinetic energy released in fission. The fission products trajectory was drawn at random from an isotropic angular distribution and this direction was kept constant assuming collisions with the medium atoms were negligible. The energy loss in the medium was computed by the equation:

$$\Delta E = \int_{d_0}^{d_0+l_x} S(E)dx \qquad 4.14\ [35]$$

In the above, the stopping power, $S(E)$ is a function of depth which allows direct estimation of energy loss, ΔE of a projectile in a medium knowing the track length, l_x of the projectile in the medium. Here, d_0 is the depth corresponding to the initial kinetic energy [35].

In [35], it was observed that the elements of flux perturbation like flux depression and self-shielding do not have any significant effect for thickness equivalent to a surface density less than a few mg/cm^2. Wall effects also were found to be non-existent as it happens only when the coating takes up all the electrode length. However, self-absorption effect could be substantial as the loss of sensitivity was found directly proportional to the surface density, i.e., coating thickness. An interpretation was made as the straight trajectory of fission product assumption for the Monte Carlo tools was valid only for thin fissile coated fission chambers having low pressure and small inter-electrode gap [35].

Trama et al. published the utilization of Extended Kalman Filter (EKF) algorithm in digital signal processing for the measurement of neutron flux and reactor period for MARINE project and

for any nuclear power plant in general [61, 62]. A simulation framework was created to adjust and check the EKF model where the measurement noise was modelled based on earlier measurements and the tuning of state noise was achieved by matching metrological predefined requirements. The simulation environment was partially implemented in MATLAB and partly in ANSI C. The improvement in the results was seen in both cases of response time and accuracy for both flux and period measurements. Unique advantages were achieved as response time and accuracy deliverance were possible at all flux level according to the operator chosen stimuli. Also, this digital signal processing technique had intrinsic flexibility to average results, to produce mean and standard deviation from a selected number of simulation cases [61].

Vermeeren et al. used FCD code on the experimental campaign on sub-miniature fission chambers (SMFC's) in the in-pile irradiation rig of BR2 reactor [68]. Three sub-miniature chambers were tested in this experimentation in the high neutron flux and high gamma heating environment of BR2 – SMFC3 and SMFC4 with fissile coating while SMFC2 was just an ionization chamber without fissile deposit. The SMFC2 current accounted for cable contribution, gamma-induced ionization of the fill gas, and the delayed current due to ionization by the decay of activation products or fission fragments in the metallic parts in the sensitive zone. The current-voltage characteristic curves for SMFC2 showed gamma contribution was dominant for the positions above the core mid plane and cable contribution became dominant for position below the mid plane. The noise when compared with the SMFC4 current showed a larger contribution which is due to optimized low amount of fissile deposit in chambers to be experimented in high flux condition. The calculated neutron sensitivity for the chambers with the FCD code matched with experimental values considering the effects due to cable, gamma, and fissile deposit consumption. The linearity of response as a function of neutron flux was obtained. For the saturation curves, the

global current-voltage characteristics remained constant even for long-term performance although the saturation domain shifted to lower voltage yet the sensitivity loss was proportional to fissile mass consumption. The experimental saturation curves showed the onset of the saturation domain was well predicted by the FCD code [68].

Cabellos et al. used the inventory code ACAB to investigate the impact of different deposits in fission chambers, effects of burnup on the concentration, impact of activation cross-section uncertainties on the fissile coting for all range of irradiation neutron fluences of interest [10]. The EAF2007[18, 74] data library which contains decay data, fission yield, activation cross-section and uncertainties were used in this study. Along with the simultaneous evolution of fission rates as a function of fluence for the fissile deposits, the long-term performance of fission chambers considering sensitivities to fast neutrons, total radioactivity, xenon prediction, and spectral history effect in Belgian Reactor 2 (BR2) due to changes in temperature were predicted. The Monte Carlo method embedded in ACAB was used to analyze the uncertainty propagation in fission chamber response. The uncertainties involved with Np-237 and Pu-242 were large pertaining to the uncertainties in Np-238 and Pu-243 fission cross-sections [10].

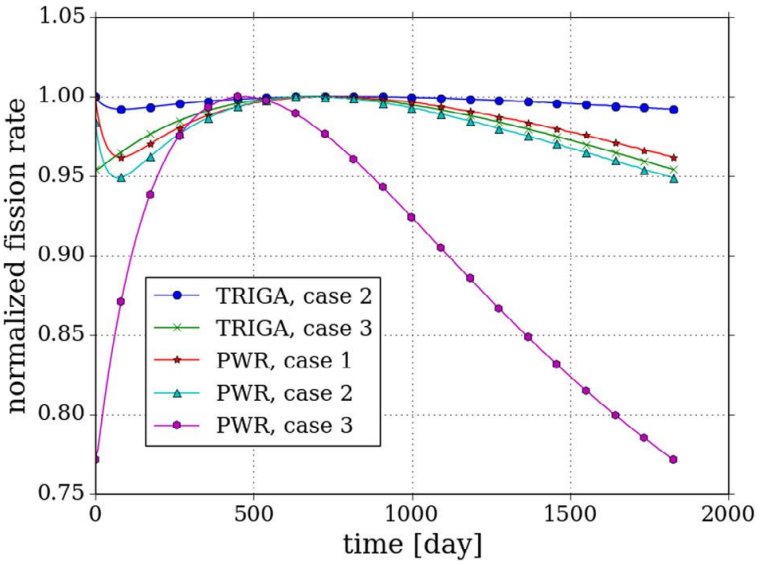

Figure 4.10: Normalized fission rate as signals as a function of time for over 5 years in a TRIGA and PWR spectrum from Reichenberger et al. [56]

Reichenberger et al. used ORIGEN-S to compute the signal (as fission rates) of MPFD's as a function of time for two types of reactor: i) TRIGA Mark II (assumed constant neutron flux of 3×10^{13} $ncm^{-2}s^{-}1$) and ii) pressurized water reactor (PWR) (assumed constant neutron flux of 3×10^{14} $ncm^{-2}s^{-}1$) with different combinations of Th-232 and U-233, U-235, and U-238 [56]. The weighted, unshielded cross-section data with appropriate energy spectra were created by utilizing ORIGEN-S. Several of the isotope compositions were tested for both reactors: 1. all four isotopes, 2. combination of Th-232, U-235, and U-238, 3. combination of U-235 and U-238. For TRIGA Mark II reactor case 1 and case 2 yielded identical compositions so only case 2 was shown in figure 4.10. The results showed that the maximum signal deviation was strongly dependent on composition and optimum composition was strongly dependent on flux spectrum. Smaller deviation in the signal for TRIGA Mark II were observed than that of PWR as the total fluence was smaller in TRIGA compared to that of PWR. It was also observed the addition of Th-232 improved the stability of the signals [56].

Chapter 5

Physical phenomena covered in modeling

5.1 Flux perturbation factors

The perturbation factors needed to be considered in case of modeling fission chambers include neutron flux self-shielding (attenuation of neutrons inside the deposit from the deposit itself), self-absorption (stopping of fission products inside the deposit), wall effect (fission product stopping in chamber walls) [25, 33, 35].

Geslot et al. suggested that signal loss due to self-shielding of neutrons and auto-absorption of fission fragments could get considerable as the thickness of the fissile coating for a fission chamber was increased [24]. An additional co-efficient, k_a was introduced to account for these two physical phenomena so that:

$$N_a = k_a \cdot N \qquad 5.1\ [25]$$

The relationship of the fission rate, R of the fissile deposit of the chamber with the ambient neutron flux Φ and with the total fission cross-section, Φ:

$$R = N \cdot \bar{\sigma} \cdot \Phi \qquad 5.2\ [25]$$

Here, N_a and N were the number of fissile atoms present in the active mass (considering only the fission products that contribute to the signal) of the fissile deposit with and without the consideration of perturbation effect respectively. The active fission rate was then,

$$R_a = N_a \bar{\sigma} \Phi R_a \qquad 5.3\ [25]$$

This reaction rate is the only possible link for the measurement of perturbation. Although, this research presented the idea of effects of self-shielding and self-absorption on the sensitivity loss of the fission chambers, it assumed this effects are negligible.

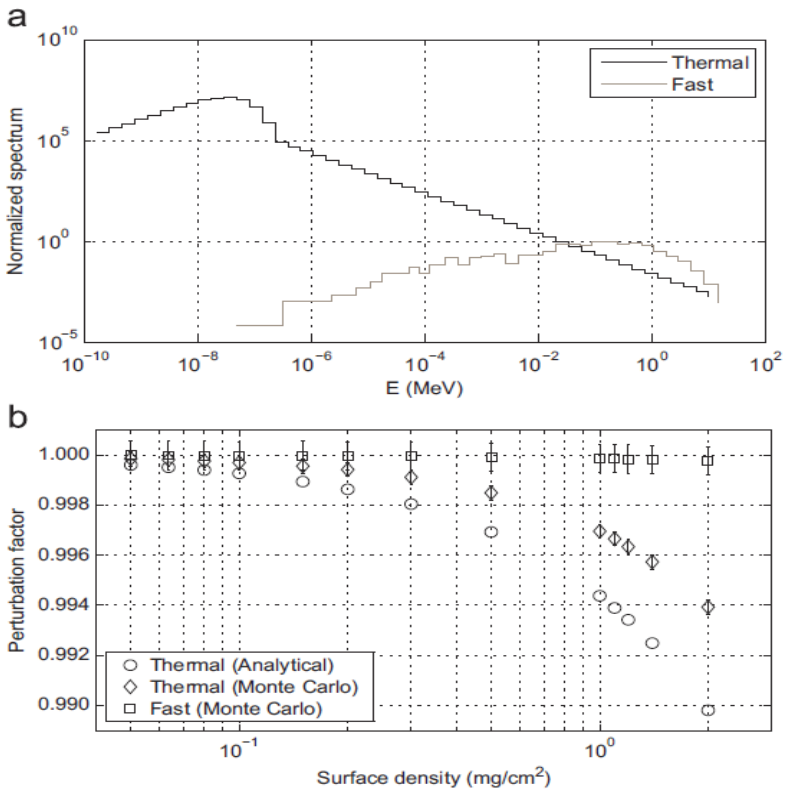

Figure 5.1: (a) The thermal and fast spectra considered to calculate perturbation factor, (b) Perturbation factor calculated for thermal and fast spectra from Jammes et al. [35]

Jammes et al. presented a thorough study on the effect of perturbations (flux depression and self-shielding) on the assumed decline in detection efficiency of a fission chamber [34]. The total perturbation factor of the chamber assuming a slab-size deposit and planar semi-isotropic neutron source parallel to the slab surface,

$$F = \frac{\int_v \int_{\partial\Omega} \int_{\partial E} \Sigma(E)\Phi\left(E,\overrightarrow{\Omega},\vec{r}\right) d^3r\, d^2\,\Omega\, dE}{\int_v \int_{\partial\Omega} \int_{\partial E} \Sigma(E)\Phi_0\left(E,\overrightarrow{\Omega},\vec{r}\right) d^3r\, d^2\,\Omega\, dE} \qquad 5.4\ [35]$$

where, F was defined as the ratio of fission reaction rates with perturbed neutron flux (Φ) to the unperturbed one (Φ_0), Σ denoted the macroscopic cross-section, V denoted the volume of the medium. MCNPX2.5 with the ENDF/B-VI neutron data library was used to calculate F of equation 5.4 to assess the impact of the fissile deposit thickness of a fission chamber. Figure 5.1(b)

shows the perturbation factor found to be ≈ 1 (always greater than 0.99) for any surface density less than 2 mg/cm^2 [35].

The physical interpretation can be given as the neutron mean free path in the type of fissile deposit used (U_3O_8) is about 10^2 order higher than the usual coating thickness of the fission chambers. So, the self-shielding effect is negligible in case of the fission chamber detection efficiency.

For the thermal spectrum, the self-shielding factor, G was calculated analytically with the following formula for a pure absorbing medium and isotropic flux,

$$G = \frac{1-2E_3(\Sigma d)}{2\Sigma d} \qquad 5.5 \text{ [35]}$$

where, $E_3(x)$ is a generalized exponential integral function of the third order (appendix of [4]), and Σ and d were the cross-section and thickness of the absorber. The analytical results were in good agreement with MCNP calculations [35].

In case of a pure absorber, G represents the probability that the neutrons entering the sample will not be captured or the neutrons that will escape capture [35]. Equation 5.5 can be derived following the same steps presented by Bell in [4] to calculate escape probabilities in the chord method by assuming a slab of fissile deposit of thickness, d and total cross section, Σ. The analytical results found were in good agreement with MCNP calculations.

The depletion issue in case of flux perturbation effect rises next. The CEA reference depletion code DARWIN calculations showed enriched U-235 (> 92% enrichment) decreased only 0.5% at best for a thermal fluence greater than 10^{19} n cm^{-2}. So, it was concluded that the self-shielding effect was non-existent during deposit depletion.

In another research where Filliatre et al. investigated Pu-242 as the optimum choice to monitor fast component of the flux, it was mentioned that the choice of the thickness of the fissile

deposit should not be arbitrary as it could affect efficiency with self-shielding and auto-absorption effect [22]. In their case, they worked with a deposit thickness less than $5x10^{-6}$ cm on an electrode with a diameter of 0.7 mm and length 8mm. The resulting interaction probability was less than $3x10^{-3}$ and so self-shielding phenomenon was not considered here. Furthermore, the TRIM code evaluation showed 99.3% of the active mass (the fission product emitted toward the gas) escaped getting absorbed within the deposit. Hence, self-absorption effect was also neglected in this case [22].

Cabellos et al. in their research on the assessment of fissionable material behavior in fission chambers analyzed the effect of the self-shielding phenomenon [10]. If Σ_{total} is the total macroscopic cross-section in cm^{-1},

$$\Sigma_{total} = \Sigma_i^N = \sigma_{total}^i N^i \quad \text{5.6 [10]}$$

where, σ_{total}^i is the total microscopic cross-section in cm^{-1}

N^i is the atomic density for isotope i in $atms/cm^3$

N is the total number of isotopes in the deposit

If the density of the fissile deposit is $\rho^{deposit}$ in gm/cm^3,

$$\Sigma_{total} = \rho^{deposit} N_A \frac{\Sigma_{i=1}^N \alpha^i \sigma_{total}^i}{\Sigma_{i=1}^N \alpha^i A^i} \quad \text{5.7 [10]}$$

Where, α^i is the fraction for isotope i in the deposit

N_A is the Avogadro number

A^i is the atomic weight of isotope i

If δ denotes the deposit thickness, the interaction probability in the deposit thickness,

$$\varepsilon = \Sigma_{total} \cdot \delta \quad \text{5.8 [10]}$$

The predicted maximum thickness for an assumed interaction probability,

$$\delta^{max} < {}^{\varepsilon}/_{\Sigma_{total}} \qquad 5.9\ [10]$$

For, all actinides (Th232, U235, U238, Np237, Pu238, Pu240, Pu242), either pure or compositions, the ACAB code evaluations showed with a usual fissile deposit thickness (~50 nm), ε values are negligible (~0.001) for fluences up to 10^{22} ncm^{-2} within the BR2, DEMO magnetic fusion reactor, and IFMIF high flux test module environment (Figure 5.2) [10].

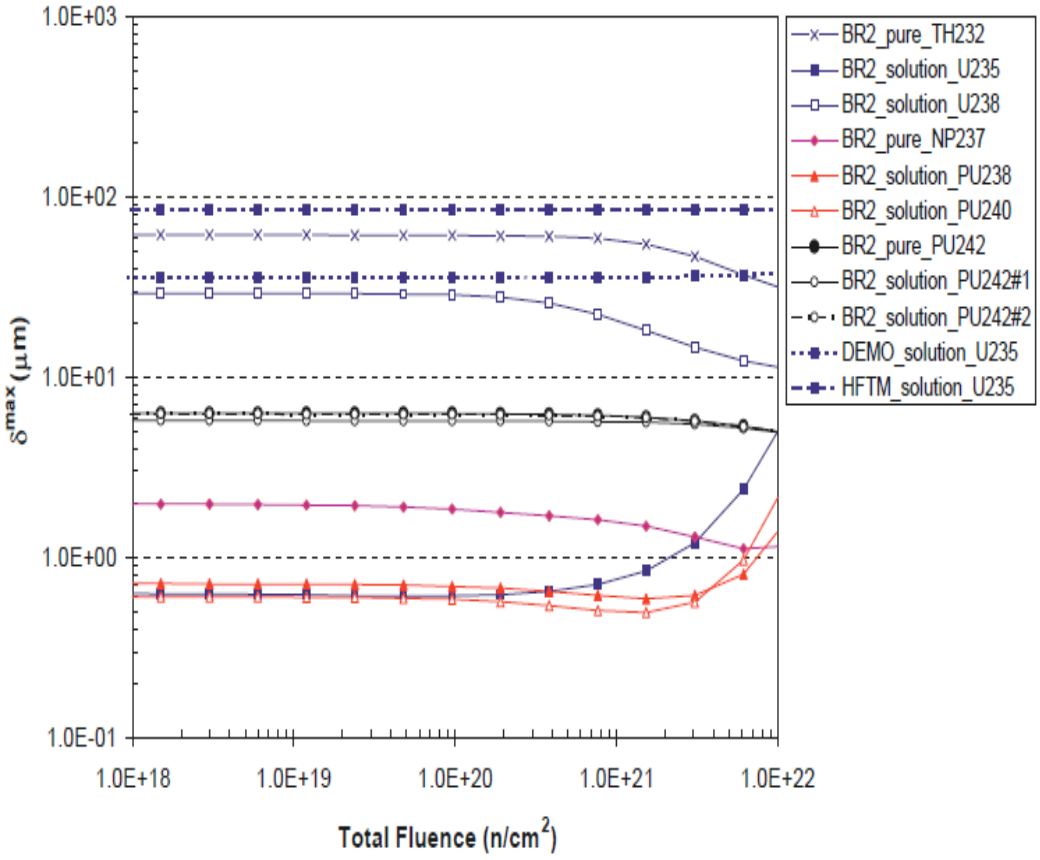

Figure 5.2: ACAB code prediction for maximum thickness for an interaction probability, $\varepsilon = 0.001$ from Cabellos et al. [10]. The isotopic compositions for Pu-242#1 Pu-242#2 are the same as presented in Table 5.1.

The self-absorption effect, i.e., the loss of fission product kinetic energy can be prominent when the fissile deposit thickness exceeds 2 mg/cm^2 [35]. Jammes et al. mentioned that the effect

of self-absorption on the sensitivity loss depended on the mode of operation of the fission chambers. The signal loss in the pulse mode due to self-absorption happens for the active fissile products absorbed within the coating or reach the gas without sufficient energy and cannot be distinguished from the noise. For current and Campbelling mode, additional to the previously expected effects, another term accounting for all the fission products losing a fraction of their kinetic energy in the deposit needs to be considered. In this research, a Monte Carlo based simulation approach was utilized to compute the self-absorption fraction and the expected fission chamber spectrum for different fissile deposit thickness [35]. The Monte Carlo tool developed in [35] was described in chapter 4 of this report. In this chapter, the results and interpretation will be presented.

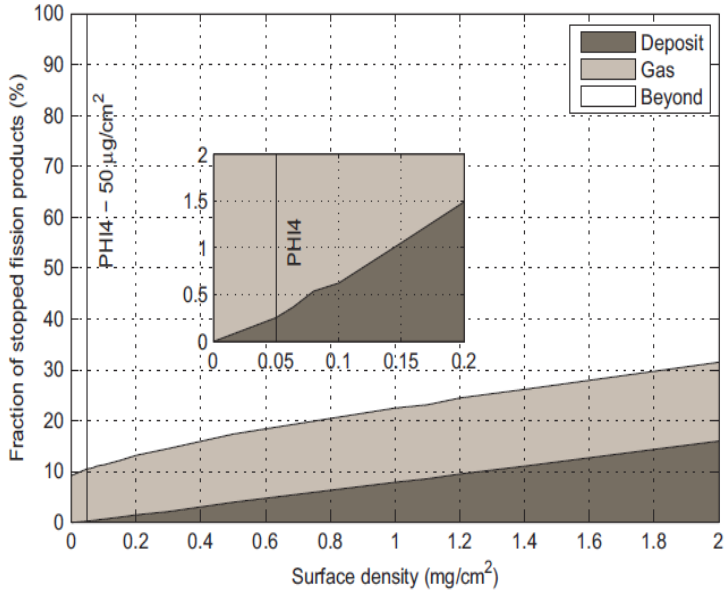

Figure 5.3: Fraction of stopped fission products as a function of varying thicknesses from Jammes et al. [35]

To find the thickness impact on the simulated fission chamber spectrum, Monte Carlo simulation with 10^5 fission product histories were done for 14 different fissile deposit thicknesses with varying surface densities (0 – 2 mg/cm^2). Figure 5.3 shows the fraction of stopped fission

products within the deposit, gas, and within cathode. The relationship between the sensitivity loss and the deposit thickness is almost linear with a slope of 8%/mg/cm^2. As the density approaches near 2 mg/cm^2, the sensitivity loss due to self-absorption can be quite substantial (~16%). The relative uncertainty loss ranges from ~7% for the lowest value of surface density (0.05 mg/cm$^{2)}$ to ≤1% for the highest value (2 mg/cm^2) [35].

Cabellos et al. in [10] to assess the effect of self-absorption utilized an empirical relationship between the average kinetic energy of the fission fragments and the mass and charge of fissioning nuclei:

$$\langle K \rangle = \frac{0.1178 Z^2}{A^{1/3}} + 5.8 \qquad 5.10\ [10]$$

where, $\langle K \rangle$ is the average kinetic energy in MeV of the fission product

Z and A are the atomic and mass number respectively of the fissioning nucleus

The stopping power (unit MeV/μm) can be predicted by SRIM at a given deposit thickness for $\langle K \rangle$. For typical deposit thickness, the stopping power was not found significant and the self-absorption effect was neglected [10].

Another source of perturbation can be wall effect which arises due to fission product stopping in the chamber walls. The Monte Carlo tool developed by Jammes et al. [35] was utilized to inspect this effect. It was found wall effect was more prominent only when the sensitive length was in tight contact to the chamber walls, i.e., the whole electrode length was deposited with fissile materials (Figure 5.4) [35].

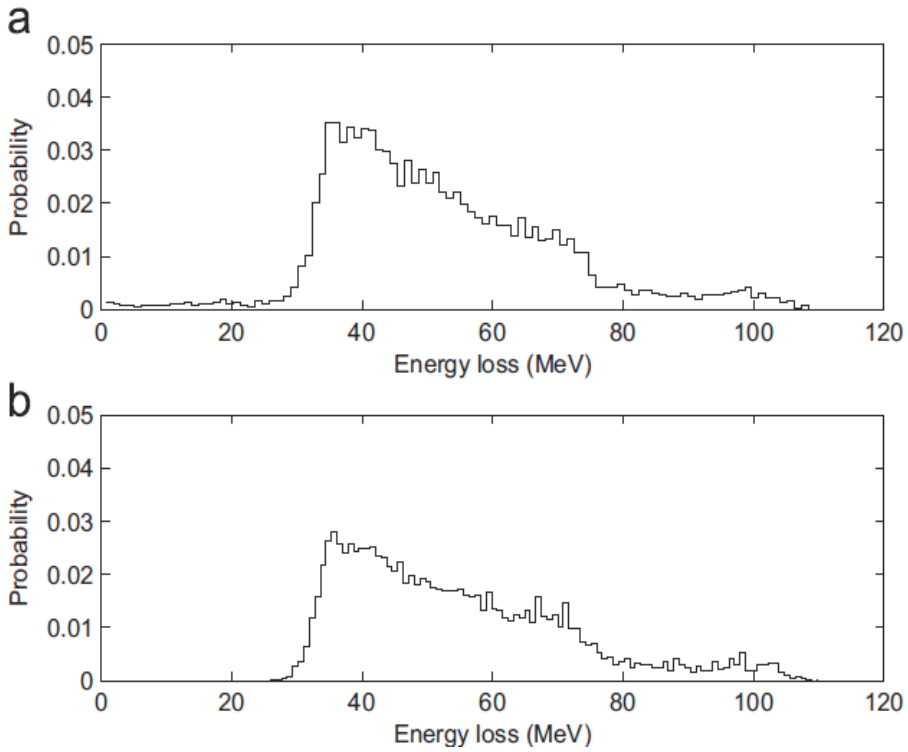

Figure 5.4: Wall effects from Jammes et al. (a) Electrode length: 8 mm, Sensitive length: 8 mm, (b) Electrode length: 12 mm, Sensitive length: 8 mm [35]

5.2 Fissile deposit evolution

The simulation of deposit evolution with DARWIN code found in the research of Filliatre et al. and Jammes et al. under Fast Neutron Detector System (FNDS) project [20, 22, 33] was already mentioned in Chapter 4 of this report. The thorough study of isotopic evolution on various isotopes established Pu-242 as the best candidate to monitor fast neutron flux for a fluence ranging from 10^{20} to 10^{21} ncm^{-2} for a Material Testing Reactor (MTR) spectrum containing both thermal and fast components. Figure 5.5 shows the sensitivity to fast neutrons, S_{fast} for initially pure deposits. It is obvious from this figure that Pu-242 is highly sensitive to fast neutrons over the whole fluence range [20, 22, 33]. Two isotopic compositions of Pu-242 (Pu-242 #1 and Pu-242 #2) were tested and among them Pu-242 #2 which contained lower amount of impurities like Pu-239 and Pu-241, showed better sensitivity to fast neutrons over the total fluence range (Figure 5.6).

The atomic percentages for two Pu-242 isotopes are shown in Table 5.1. If Pu-242 #2 was left for 25 years before irradiation, its performance was significantly improved because Pu-241 was a β^- emitter with a half-life of 14.35 years [20, 22].

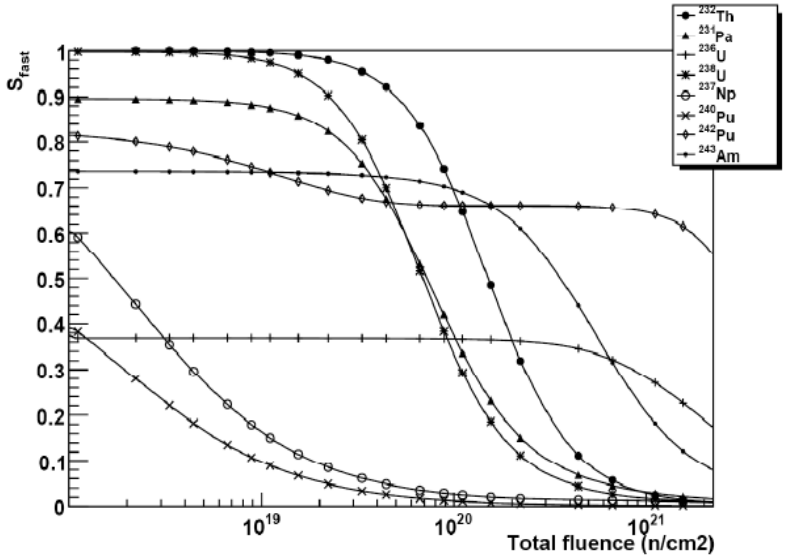

Figure 5.5: Sensitivity to fast neutron for different pure isotopes from Filliatre et al. [22]

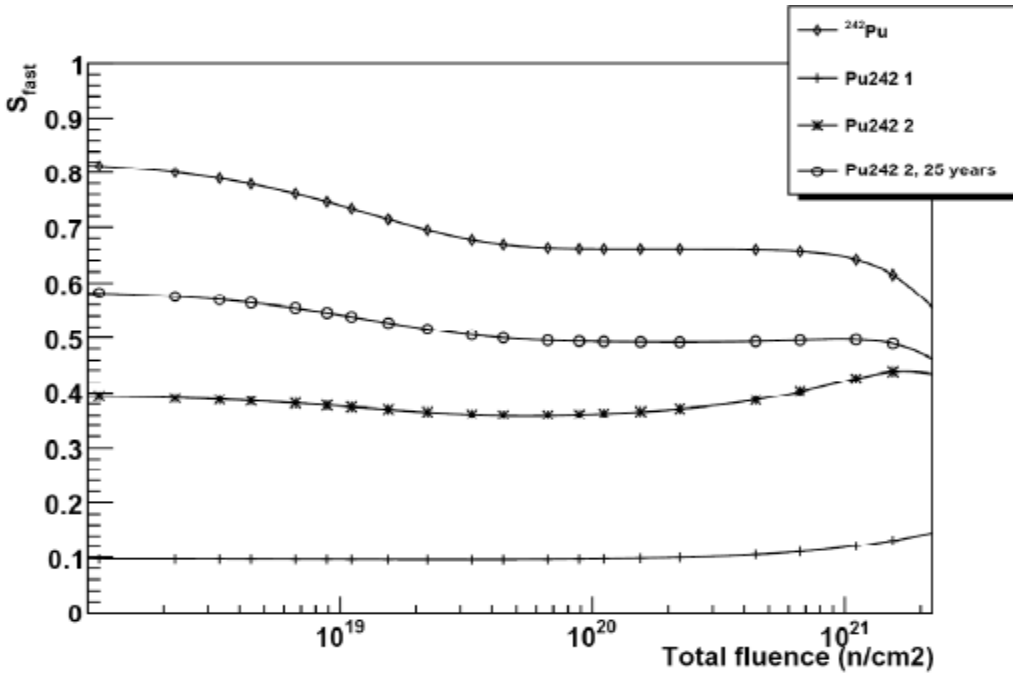

Figure 5.6: Sensitivity to fast neutrons for i) Pure Pu-242, ii) Pu-242#1, iii) Pu-242#2, iv) Pu-242#2 left for 25 years before irradiation from Filliatre et al. [22]

Table 5.1: Isotopic compositions in atomic percentage for Pu-242#1 and Pu-242#2 from Filliatre et al. [22]

	Pu-238	**Pu-239**	**Pu-240**	**Pu-241**	**Pu-242**	**Pu-244**
Pu-242#1	0.214	0.116	0.017	0.180	99.274	0.044
Pu-242#2	0.004	0.005	0.022	0.035	99.932	0.002

Fissile deposit evolution using other evolution codes like EVO77 and CINDER was discussed in detail in chapter 4.

5.3 Gas behavior under irradiation:

Fission chambers are supposed to operate in high irradiation condition so some basic requirements are using inert gases for fill gas maintaining a pressure usually near 1 bar. The use of inert gas is because of avoiding gas degradation through dissociation reactions under irradiation. High values of gas pressure are avoided since they will increase gas escape in the irradiation system [15]. Yet, some predicaments of gas behavior under irradiation cannot be avoided.

Jammes et al. mentioned that, the quenching process, i.e., addition of CO_2, CH_4, or N_2 with the filling gas could help minimizing the charge collection time but there existed the risk of decomposition of these gases under irradiation and or getting combined with fission chamber materials [34]. The fill gas of the fission chamber tested was argon with 4% nitrogen. The experimental observation was that the nitrogen molecules started to disappear under irradiation with the rising temperature and were completely removed after 3000 hours at a temperature near 550◦C - 600◦C [34].

Under irradiation, the monoatomic fill gas can get polluted by the generation of volatile fission products [42]. These additives and contaminants can lead to Penning effect [34, 42] for which changes can happen in the basic properties of the fill gas. If the excitation energy of the metastable states of the principle gas is larger than the ionization energy of the impurities or the

gaseous additives, the collision between these two will ionize the impurities or the additives. The result is the reduced effective ionization potential of the fill gas. The initial sensitivity loss under irradiation by the degradation of the fill gas resulting from the outgassing by the chamber component, mainly the anode with fissile deposit, at a temperature of 300◦C was reported by Oriol et al. [49]. From the manufacturing point of view, this problem of gas evolution under irradiation can be solved by degassing the chamber components including the deposit and or by nitriding (saturate all the chamber components with nitrogen) [34, 47]. Fadil et al. [19], Letourneau et al. [42] recommended using gases like He or Ne that have higher ionization potential than Ar as fill gas for higher neutron flux environment. The possible problem like Jesse effect (in presence of small amount of impurities the secondary ionization in gases with higher ionization potential can be significant) was also mentioned. Scarcity in modeling of gas behavior under irradiation considering Penning and Jesse effect was observed.

The most significant problem of gas behavior under irradiation found by Chabod et al. in their work of analytical approach to the modeling of fission chambers in current mode was mentioned briefly in chapter 4. It was found that the addition of contaminants with low ionization potentials such as xenon to the fill gas would promote secondary ionization. The result is the shift of avalanche towards lower voltages and the catastrophic consequence on the saturation plateau [13]. Xenon is one of the most abundant fission products of U-235. The experimental observation is that for a standard fission chamber with argon at a pressure of 1 bar, for a 4 µg U-235 deposit, within 10^{15} $ncm^{-2}s^{-1}$ thermal neutron flux, the contamination of 0.1% in xenon shifts the initiation of avalanche by 20V (Figure 5.7) [13, 15].

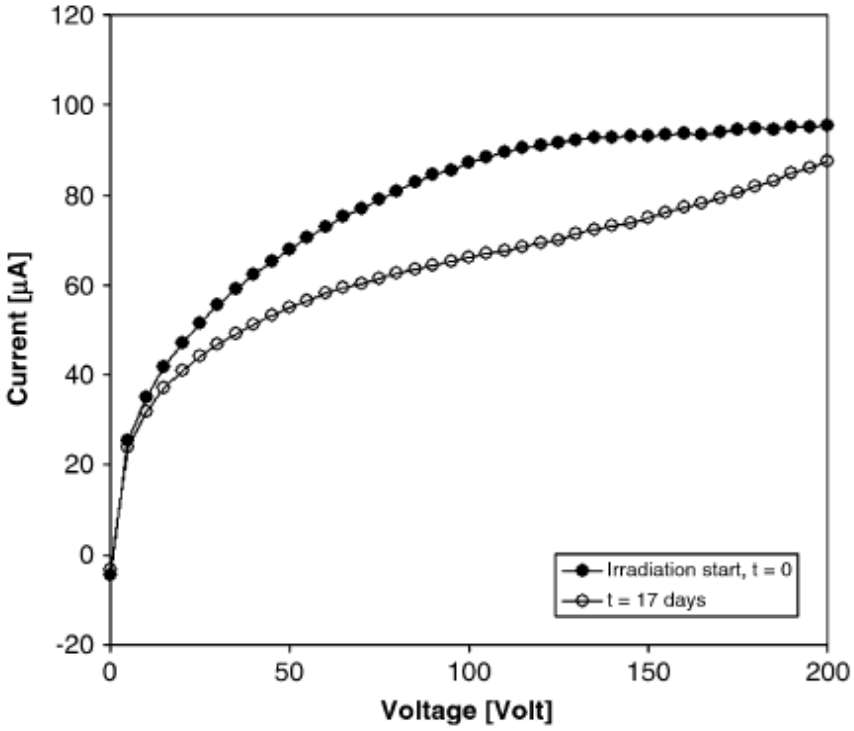

Figure 5.7: Evolution of the experimental calibration curve shapes of the fission chamber with 98.5% pure U-235 deposit during irradiation at ILL/Grenoble High-Flux Reactor from Chabod et al. [13]

Cabellos et al. computed the total isotopic concentration of xenon due to fission reaction in the fission chambers during irradiation by ACAB code (Figure 5.8) [10]. For deposits like U-235, Np-237, Pu-238, Pu-240; levels higher than 10^{16} atoms of xenon were obtained in BR2 reactor. Levels within 10^{15} to 10^{16} were found for U-238 and Th-232 deposits in BR2 reactor, U-235 and Pu-238 for DEMO reactor and Pu-238 for HFTM [10].

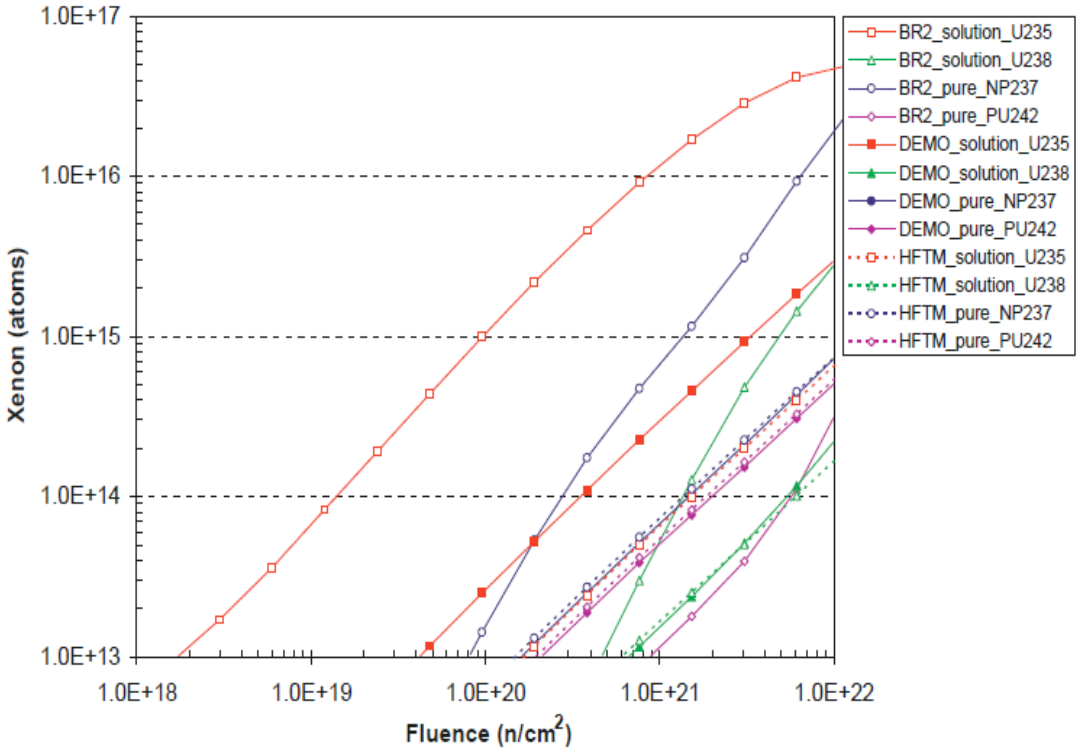

Figure 5.8: Xenon contamination in the fill gas in the fission chamber for initially different pure (Np-237 and Pu-242) and solution (U-235 and U-238) deposits in typical high neutron flux environments from Cabellos et al. [10]

If the choice of gases like He or Ne with higher ionization potential than that of Ar is adopted for fill gas, another phenomenon named Jesse effect (minute amount of contaminant will enhance ionization significantly) can arise [10, 42]. Chabod et al. recommended keeping the inter-electrode space to facilitate the measurements while avoiding perturbations that arises in high neutron flux environment [13].

Filliatre et al. in their research on Monte Carlo simulation for the pulse shape of the fission chambers assumed that fill gas was homogeneous and did not evolve under irradiation [23]. In [21], the research on joint estimation of the fast and thermal components of a high neutron flux

with dual detectors, Filliatre et al. indicated that more comprehensive studies of modeling of fission chambers could be done by considering the evolution of the gas composition.

5.4 Electron-ion pair creation:

Filliatre et al. in their research of the simulation of fission chamber pulse shape by GARFIELD described how the electron-ion pair creation was treated in case of modeling [23]. On an average, a fission product generates about 10^5-10^6 electron/ion pairs. It was estimated that the number of histories must be about 10^4 in order to attain good statistics. To save the computation time, the electron-ion pairs are generated in clusters within the GARFIELD code where the maximum number of clusters is user-tunable [23].

The average number of electron-ion pairs in cluster, i is given by:

$$N_i = \frac{2E}{Wm_x} \qquad 5.11 \text{ [23]}$$

where, E is the initial kinetic energy of the fission product.

W is the average energy needed to create one ion pair

m_x is the maximum number of clusters

The average distance between the clusters,

$$d_i = N_{cl} \frac{W}{dE/dx} \qquad 5.12 \text{ [23]}$$

The position of each cluster depends on the direction of the fission product, the average distance between the clusters, and the longitudinal and lateral straggling. A straight-line trajectory for the fission product direction was assumed. For each cluster, the fission product energy is reduced by $N_i W$ on an average [23]. As mentioned in chapter 4 of this report, larger histories per cluster is needed to avoid clustering bias.

A similar approach was taken for charge pair creation by Jammes et al. with GARFIELD simulation although the cluster method was not mentioned [33].

5.5 Charge transport:

The charge conservation equations for a generic fission chamber are:

$$\frac{\delta n_e}{\delta t} + div(\rho_e \langle v_e \rangle) = t^e_{source} + t^e_{loss}$$

$$\frac{\delta n_a}{\delta t} + div(\rho_a \langle v_a \rangle) = t^a_{source} + t^a_{loss}$$

5.13 [13]

where, $\frac{\delta n_e}{\delta t}$ and $\frac{\delta n_a}{\delta t}$ denotes the rate of change of electrons and fill gas ions, respectively.,ρ_e and ρ_a are the electron and ion densities, $\langle v_e \rangle$ and $\langle v_a \rangle$ are electron and ion average drift velocities, and t_{source} and t_{loss} are the source and loss terms which represents the charge pairs created and destroyed per unit time inside the chamber [13].

Based on these equations Chabod et al. described the analytical method of charge transport for cylindrical geometry fission chambers [13].

The temporal derivatives will vanish in equation 5.13 as chambers in current mode work in a stationary state.

$$div\left(\rho_e \langle \underline{v_e} \rangle\right) = t^e_{source} + t^e_{loss}$$

$$div\left(\rho_a \langle \underline{v_a} \rangle\right) = t^a_{source} + t^a_{loss}$$

5.14 [13]

If the applied voltage between the anode and cathode is ΔV, an electric field $\vec{E}$ that obeys Maxwell-Gauss equation arises. For cylindrical fission chambers, ρ_e and ρ_a depend only on radial

coordinate, r. Let, anode and cathode are two coaxial cylinders of respective radii R_1 and R_2. It can be written as:

$$\frac{1}{r}\frac{\partial}{\partial r}rE(r) = \frac{\rho_e(r) + \rho_a(r)}{\varepsilon_0}$$

$$\int_{R_1}^{R_2} E(r)dr = \Delta V$$

5.15 [13]

Since, ions drift towards cathode and electrons drift towards anode, it can be written as:

$$-\frac{1}{r}\frac{\partial}{\partial r}r\rho_e v_e = t^e_{source} - t^e_{loss}$$

$$\frac{1}{r}\frac{\partial}{\partial r}r\rho_a v_a = t^a_{source} - t^a_{loss}$$

5.16 [13]

where, v_e and v_a are respectively the average radial projections of the electron and ion velocity.

The disappearance of an electron involves disappearance of an ion, so the absolute values of the creation and loss terms for the electrons and ions can be treated equal.

$$\rho_e = -en_e$$

$$\rho_a = -en_a$$

$$t^a_{source} = -t^e_{source} = eT_S$$

$$t^a_{loss} = -t^e_{loss} = eT_L$$

5.17 [13]

So, equation 5.6 can be written as:

$$-\frac{1}{r}\frac{\partial}{\partial r}rn_e v_e = T_S - T_L$$

$$\frac{1}{r}\frac{\partial}{\partial r} r n_e v_e = T_S - T_L$$

5.18 [13]

The output current of the chamber can be written as:

$$I = \iint_S \left(-e n_e \underline{v_e} + e n_a \underline{v_a}\right) . \underline{dS}$$ 5.19 [13]

The coupled resolution of equation 5.5 and 5.8 will help to evaluate the functions $n_e(r)$, $n_a(r)$, and $E(r)$ according to the voltage applied to the electrodes. The output current, I as a function of applied voltage, ΔV by considering the equation 5.9 for specific fission chamber geometry.

The drift chamber simulation program GARFIELD was utilized in several studies on modeling of fission chambers to deal with charge transport [23, 33]. As mentioned in chapter 4, the positive ions can be treated analytically as they are subject to Brownian motion so it is only the transport of electrons that needs the attention of computation codes. MAGBOLTZ code embedded in GARFIELD was employed to compute drift velocity of electrons and diffusion coefficients in [33]. In a cluster based GARFIELD simulation, each charge in each cluster of GARFIELD is drifted with a Runge-Kutta-Fehlberg integration method [23].

5.6 Space charge buildup, charge recombination and avalanche:

The plateau region in the fission chamber saturation curve tends to vanish at an inflexion point when the neutron flux increases (near 2-3x10^{14} ncm^{-2}s^{-1}) [42]. Letourneau et al. in their research on the developments on micrometric fission chambers for high neutron fluxes studied the origin of this effect [42].

The t_{source} term in equations 5.13 can be expanded as:

$$t_{source} = t^1_{source} + t^2_{source} \quad \text{5.20 [42]}$$

The t^1_{source} is due to ionization of the gas by the fission product (primary ionization). The t^2_{source} term arises due to secondary ionization and can be put into the following formula:

$$t^2_{source} = \alpha n_e v_e \quad \text{5.21 [42]}$$

where, α is the Townsend first ionization coefficient, n_e is electron density and v_e is the drift velocity of electrons.

The t_{loss} term in equations 5.13 can be expanded as:

$$t_{loss} = k n_e n_a \quad \text{5.22 [42]}$$

where, k is called the recombination coefficient which depends on the nature of the gas and n_a is the ion density. The t_{loss} term arises due to the recombination of electrons with ions. When the fission rate increases, the gradual disappearance of the plateau is primarily due to t_{loss} term. The drift velocity of the electrons and mainly of the positive ions are not sufficiently high to catch up with the charge collection time. The density of the ionized atoms pile up and creates the space charge phenomenon. The electric field is distorted with the decrease near anode and increase near cathode. When the voltage is increased, the field distortion gets even worse and it increases the charge collection time. The recombination extends at a higher voltage and avalanche starts at a lower voltage and the saturation plateau completely disappears [42].

Poujade et al. represented a theoretical model to help establish the saturation domain of fission chambers of any given geometry, the limit of which is controlled by space charge effects [54]. This model predicts the optimum parameters and optimum operating voltage of a fission chamber prior to its operation under intense neutron flux. The model considers all applicable

physical phenomena like primary ionization, electrical drift and temperature, recombination, threshold condition and charge collection of a fission chamber [54].

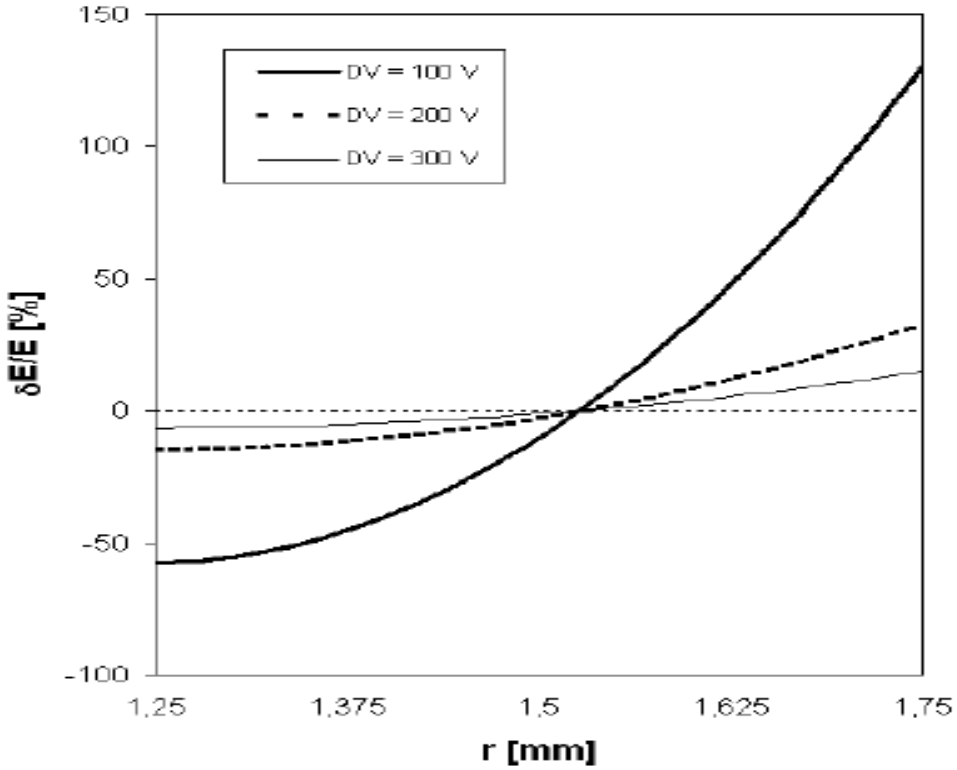

Figure 5.9: Distortion of the electrical field induced by space charges as a function of the radial distance *r* for different applied voltages from Poujade et al. [54]

The distortion of the radial electric field, δE due to space charge effect inside a cylindrical fission chamber is given by

$$\delta E(r, N_{0,}C) = \left[N_0 \frac{e}{4\varepsilon_0}\left(\frac{r^2-2r_a^2}{\mu_+} + \frac{r^2-2r_c^2}{\mu_-}\right) + \frac{C}{r^2}\right]^{\frac{1}{2}} \quad 5.23 \text{ [54]}$$

where,

r_a is the radius of anode

r_c is the radius of cathode

μ_+ and μ_- are the mobilities of the charges depending on the nature of the gas

N_0 is the density of ion pairs depending on the pressure and type of the gas

C is a constant depending on N_0 and on the interelectrode space

The calculated distortion of the radial electric field due to space charge effect at different radial distance for different applied voltage was shown in Figure 5.9.

For parallel plate configurations like MPFDs, the space charge contribution on the steady-state electric field can also be deduced in the same way as described by Palestini et al. [50]. If the positions of the anode and cathode of the fission chamber are at $x = 0$ and $x = D$ respectively and the steady-state electric field distribution is $\underline{E} = E(x)\hat{x}$, the electric field behavior around electric charges is of the same form of Maxwell's equation:

$$\underline{\nabla}.\underline{E} = \frac{dE}{dx} = \frac{\rho}{\epsilon} \qquad 5.24\ [50]$$

where, ρ is the positive charge density and ϵ is the dielectric constant of the fill gas.

From the continuity equation,

$$\underline{\nabla}.\underline{J} + \frac{\partial \rho}{\partial t} = \underline{\nabla}.\rho\underline{v} + \frac{\partial \rho}{\partial t} = K \qquad 5.25\ [50]$$

where,

$\underline{J} = \rho\underline{v}$ is the current density of the positive ions.

$\frac{\partial \rho}{\partial t}$ is the rate of change of charge density and $\underline{v}$ is the drift speed of the ions.

K is the volume rate of change of ion pairs.

The steady state solution from equation 5.24 considering the electric field and the ion velocity in the x direction,

$$\frac{d\rho v}{dx} = K \qquad 5.26\ [50]$$

Solution of equation 5.25,

$$\rho v = Kx \qquad 5.27\ [50]$$

The drift speed of the positive ions towards cathode,

$$\underline{v} = \mu \underline{E} \qquad 5.28\ [50]$$

where, μ is the positive ion mobility and it is independent of the electric field strength, $\underline{E}$.

Using the relationship of equation 5.27 in equation 5.26, if the velocity, $\underline{v} = v\hat{x}$ is interchanged with the electric field $\underline{E} = E\hat{x}$,

$$\rho = \frac{Kx}{\mu E} \qquad 5.29\ [50]$$

From equations 5.23 and 5.28:

$$\frac{dE^2}{dx} = \frac{2Kx}{\epsilon\mu} \qquad 5.30\ [50]$$

The solution of equation 5.29,

$$E(x) = \sqrt{E_A^2 + \frac{Kx^2}{\epsilon\mu}} = E_0\sqrt{\left(\frac{E_A}{E_0}\right)^2 + \frac{Kx^2}{\epsilon\mu E_0^2}} \equiv E_0\sqrt{\left(\frac{E_A}{E_0}\right)^2 + \sigma^2\frac{x^2}{D^2}} \approx E_A\left[1 + \frac{1}{2}\left(\frac{\sigma E_0 x}{E_A D}\right)^2\right]$$

5.31 [50]

where, E_A is the electric field at the anode

$E_0 = \frac{V}{D}$ is the nominal electric field in the absence of space charge.

V is the voltage difference between the anode and the cathode.

$\sigma = \frac{D}{E_0}\sqrt{\frac{K}{\epsilon\mu}}$ is a dimensionless parameter.

The approximation is true when ${}^{\sigma E_0 x}/_{E_A D} \ll 1$, i.e., $\sigma \ll 1$.

Filliatre et al. in the research of fission chamber pulse shape using GARFIELD [67] considered avalanche phenomena, but GARFIELD could not simulate recombination effect [23]. The computation of the electron-ion drift by GARFIELD, avalanche effects were included. It was suggested in this research that further work needed to be done taking into account recombination and space charge effect.

Chabod et al. in their work on the improvements of the modeling of micro fission chambers operated in current mode utilized the recombination and avalanche effect [15]. The Townsend coefficient, α, was evaluated in this research by using BOLSIG software. It was suggested in this research that the further precision of the results would need to consider the electron-ion recombination coefficient data for rare gases at successive pressure intervals [15].

5.7 Signal computation and electronic pulse shape:

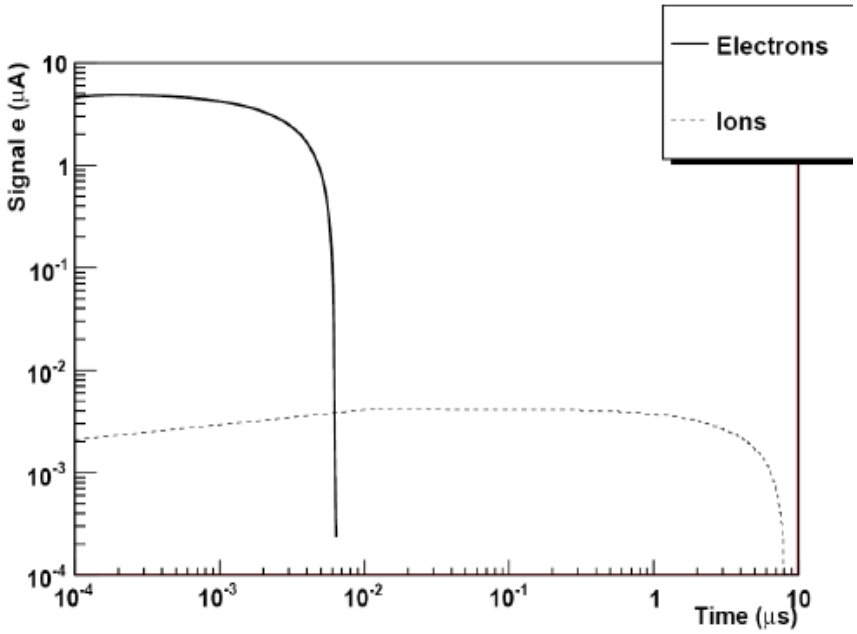

Fig 5.10: Signals due to electrons and ions (averaging over 10^5 individual signals) from Jammes et al. [33]

The procedure of simulating electric field pulse shape for a fission chamber with GARFIELD code includes random selection of a fission product and its kinetic energy, random initial direction of the fission product in the fill gas, simulation of the trajectory of each fission product with SRIM, Generation of electron-ion pairs for each interaction of the fission product with fill gas atoms, computation of the electron transport by MAGBOLTZ, sampling of the electron and ion currents at the electrodes using GARFIELD [33].

The average signal due to charge collection is shown in Figure 5.10. The pulse width of the electron component is ~10 ns whereas that of the ion component is ~10μs. This variation in timescale can create problem in their simultaneous amplification and it is recommended to filter out the ion component [33].

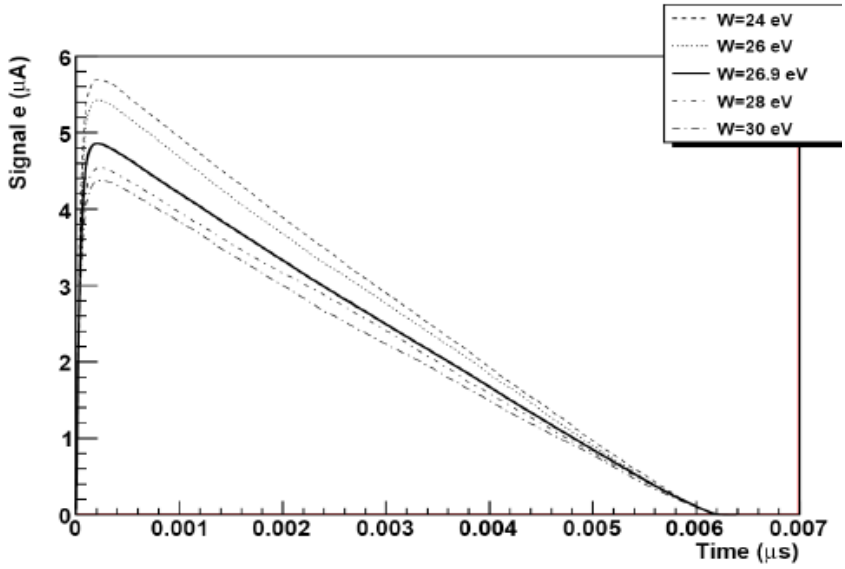

Fig 5.11: Fission chamber signals for various W-value from Jammes et al. [33]

Figure 5.11 shows that the fission chamber signals depend on W-values. The smaller the W-value, the higher the signal amplitude. This is a proof of the relationship between collected charge and W-value presented in equation 5.11. A good knowledge of W-value is essential for the exact simulation of signal amplitudes in current and Campbelling mode since the current signal is proportional to the total collected charge in current mode and in campbelling mode the signal is proportional to the square of the total collected charge [33].

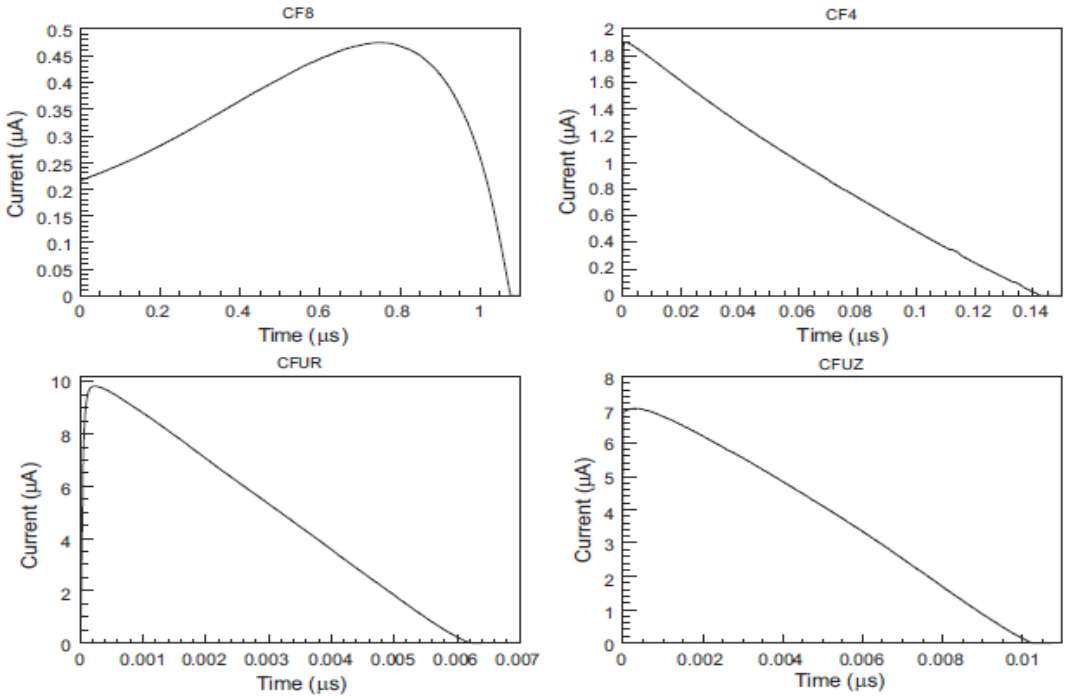

Fig 5.12: Mean electron pulse for different versions of fission chambers developed by CEA: CFUZ, CFUR, CF4, CF8 from Filliatre et al. [23]

In a cluster based signal computation by GARFIELD presented by Filliatre et al., the induced current due to the charge drift is computed as a function of time. Pulses are time sampled and retrieved by root [73] script, weighted by each cluster size, shifted in the time associated to each cluster and accumulated to produce electron and ion pulse [23]. When several CEA versions of the fission chambers were tested under this computation, it was found the chambers having smaller inter-electrode gap, could not reflect the whole energy distribution in the charge spectrum (CFUR, CFUZ in Figure 5.12, notice the difference in timescale for the four chambers). This problem is due to the physical design, not a shortcoming of the modeling. For chambers having larger gap, the charge collection was larger (CF8, CF4 in Figure 5.12). The pulse shapes were triangular for all chambers except for the cathode-coated chamber which had an inverted pulse

shape compared to the others (CF8 in Figure 5.12). The ion collection time was found three orders of magnitude greater than the electron collection time [23].

The utilization of extended Kalman filter (EKF) algorithm [58] for digital signal processing for MARINE project was discussed in chapter 4. The filtered Poisson process for signal modeling and processing developed by Elter et al. [17] was also discussed in chapter 4.

5.8 Propagation of electronic pulse through electronics:

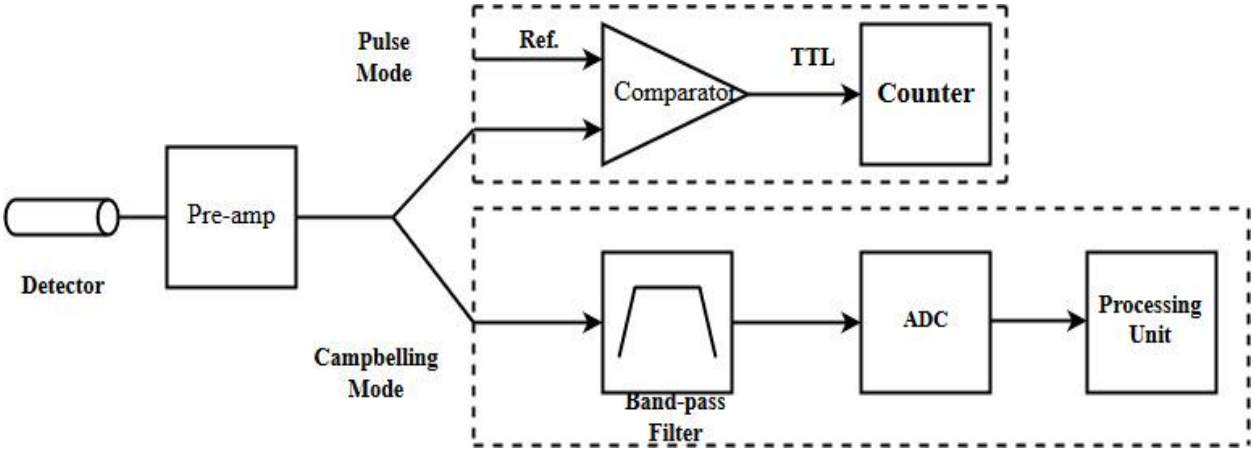

Figure 5.13: Sketch of a neutron monitoring system for pulse and Campbelling mode, picture adopted from Elter et al. [17]

A typical neutron flux-monitoring system electronics consists of the detector chamber itself, a high electromagnetic immunity cable and a preamplifier with much lower input impedance than that of the detector to convert the current flowing through the detector to a measurable voltage. Elter et al. presented the overall layout of the neutron monitoring system for pulse and Campbelling mode [17]. The pulse mode acquisition consists of a discriminator or comparator connected to the counter to check if the incoming signal falls into the predefined window or range. The counting process is achieved by a transistor-transistor logic (TTL) where the discriminator

will produce a logic signal based on the input. The Campbelling mode acquisition system includes a frequency band-pass filter, analog-to-digital (ADC) converter, and a processing unit for variance calculation [17].

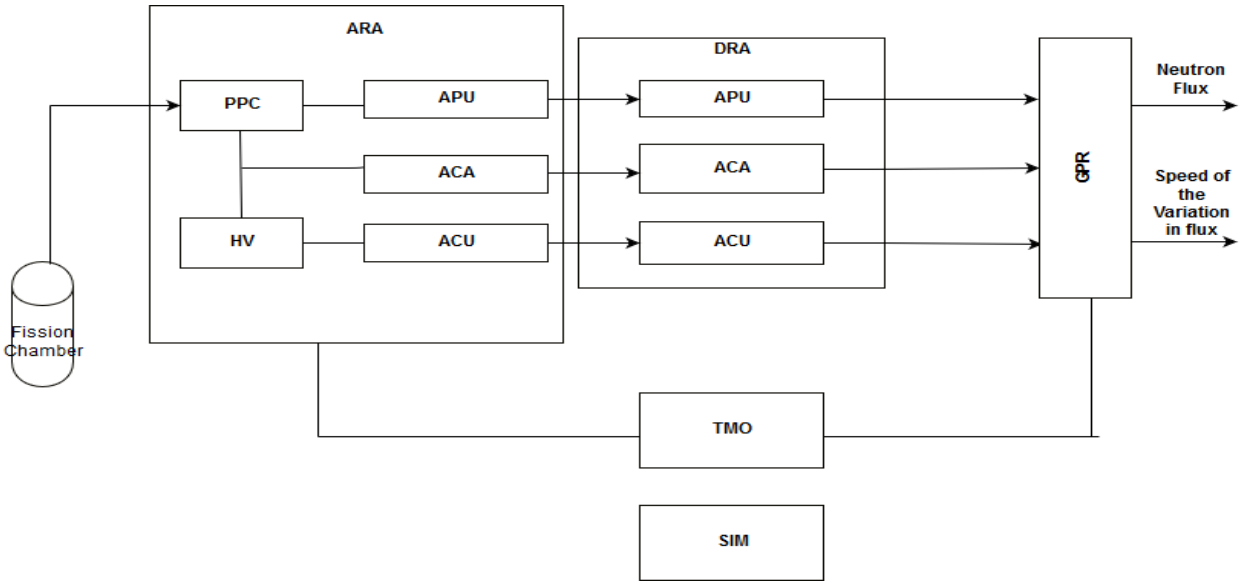

Figure 5.14: Sketch of the overall neutron monitoring system concept of MARINE project, adopted from Trama et al. [62]

Table 5.2: Acronyms used for MARINE monitoring concept, adopted from Trama et al. [62]

Acronym	**Full Form**
ARA	Analog RAck
APU	Analog PUlse mode conditioning unit
ACA	Analog CAmpbell mode conditioning unit
ACU	Analog CUrrent mode conditioning unit
PPC	Preamplifier Pulse and Campbelling
HV	High Voltage
DRA	Digital RAck
DPU	Digital PUlse mode preprocessing unit
DCA	Digital CAmpbell mode preprocessing unit
DCU	Digital Current mode preprocessing unit
GPR	Global Processing unit
TMO	Test MOdule
SIM	SIMulator

The project MARINE (French acronym for automated neutron measurement) under CEA and Technicatome used the linear electronics together with an early signal digital conversion followed by specifically designed signal processing techniques [38, 59]. The research introduced a novel digital wide range (12 decades) ex-core neutron monitoring system to overcome the traditional analog line drawbacks and to enhance "the transient response time versus accuracy compromise (TRTAC)" when providing neutron flux and reactor period information. The general concept of MARINE involved a neutron sensor (an ex-core fission chamber) producing signals in pulse mode for low range, Campbelling mode for the intermediate range, and current mode for the higher range. The Analog Rack (ARA) whose input stage is a current preamplifier then conditioned the analog signal to send it to the Digital Rack (DRA) for the digital production of the raw estimate of the neutron flux. The global processing unit (GPR) which offered the man-machine interface and the measurement data backup computed the final flux estimate and the speed of the variation in flux. A test module (TMO) took command from the GPR and did on-line tests of the sensors and of the electronics. The final stage is the computerized simulator (SIM) written in MATLAB and partly in ANSI C developed, validated, and tuned all the numerical codes of DRA and GPR. The prototype built successfully passed the tests delivering better performance compared to existing ones in terms of TRTAC, modular electronics, digital signal processing, lower maintenance cost [42, 62].

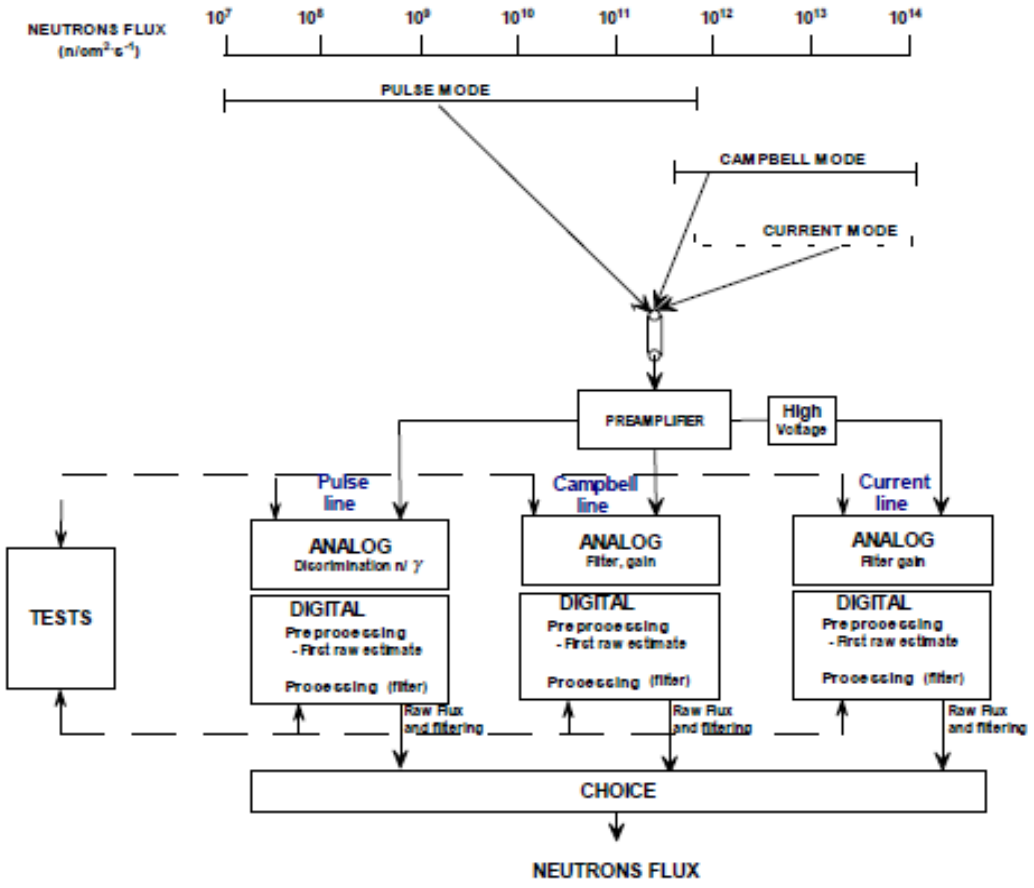

Fig 5.15: Sketch of the IRINA monitoring system electronics from Normand et al. [46]

The extension of MARINE project was IRINA involved a small diameter in-core wide-range fission chamber able to work within the range of 10^7 – 10^{14} $ncm^{-2}s^{-1}$[46]. A simulation code was written in MATLAB for the optimization of the detector. The code could calculate the sensitivity of the detector in all three modes (pulse, Campbelling, and current) considering space charge effect for high flux condition. The maximum neutron flux was settled for the detectors keeping in mind the electric screening effect as the detector linearity could be hampered with even only 4% screening of the nominal field. To check the reliability of the code it was first tested with the two previously built detectors. The order of the experimental and simulated sensitivity matched for all

three modes. Two test detectors were built varying the coating mass and gas pressure to operate in the expected neutron flux range with pulse sensitivity of 10^{-5} pulse/n.cm^{-2}s^{-1}. The simulation and experiment results show a good agreement and the detectors were able to operate up to 10^{14} ncm^{-2}s^{-1} at room temperature with a 250 V bias. The discrimination curves showed the detectors had high signal to noise ration and the saturation curves showed they operated in the saturation/ionization mode for the whole range. The next step would be to test the simulation with a higher temperature. In a temperature like 310◦C, the gas pressure inside the detector was supposed to increase and the resultant space charge buildup could affect the non-linearity of the detectors [46].

Chapter 6

Conclusion

The advancement in near-core and in-core fission chamber technology led to the development in fission chamber modeling from various aspects. Huge improvement in modeling and simulations of miniaturized fission chambers took place in recent years [7, 8, 10, 13, 14, 17, 20, 21, 22, 23, 33, 35, 54]. Several researchers from France, e.g., Chabod et al., Poujade et al. came up with detailed mathematical formulae to model the saturation current of fission chambers. A number of researchers presented higher order statistical techniques to treat the Campbelling operational mode which is of great interest in obtaining better gamma discrimination and improvement in the signal [16, 43, 52]. The recent researches indicated the need to consider most of the physical phenomena inside fission chambers to improve the simulation of fission chamber signal. Many contemporary simulation and computation processes considered neutron-flux self-shielding, self-absorption, space charge build-up effects. Research work in a good number were found in case of modeling pulse shape and propagation of electronic pulse through several electronics. Computer codes like DARWIN, EVO77, ACAB dedicated to fissile deposit evolution were utilized in different projects of finding most suitable fissile deposit for specific system and objectives or in actinide transmutation studies. The development of a single code like CHESTER devoted to capture all physical processes inside a fission chamber is a notable improvement [26]. There are some areas that still need attention in case of the development in fission chamber modeling. Effects related to gas performance improvement, i.e., Penning and Jesse effect needs to be considered. There should be more research on modeling the evolution of gas behavior under irradiation. Computer codes based on higher order statistics for fluctuation mode needs to be developed. Development of single codes for chamber modeling like the CEA in-house one,

CHESTER can be thought of. It was observed uncertainties in the nuclear data provided by the evaluated nuclear data libraries [18, 39] results in uncertainty in the computation. Methods needs to be developed to estimate this uncertainty due to provided data (the work of Cabellos et al. [11] can be exemplary in this case) and uncertainties associated with each stage of fission chamber modeling.

This report focused on the modeling and simulation of the miniature and sub-miniature designs developed by CEA. CEA developed fission chambers exhibited good performance under high flux conditions. But these commercially available coaxial cylindrical designs have problems of survivability under reactor transients. The gas leakage due to welding failure and the de-bonding issue of fissile deposits during transient pulsing were reported by Carpenter et al. and Unruh et al. [12, 66]. MPFDs showed better performance in this case and these detectors are of particular interest as in-core monitoring instruments in Transient Reactor Test Facility (TREAT). Although MPFDs are based on the same concepts as coaxial cylinders, these detectors employ two parallel plates as electrodes housed on temperature and radiation resistant ceramics. MPFD signal does not depend on the full energy deposition of the fission fragments within the interelectrode space. Because of these characteristics, MPFDs can operate with a smaller size and lower fill gas pressure which enables these sensors to survive the harsh conditions of reactor transients. In recent years, Reichenberger et al., Patel et al. published works on MPFD modeling corresponding to the recent improvements of MPFD designs [51, 55, 56]. The trends observed in the modeling and simulation of CEA developed miniaturized chambers will come useful for future modeling of MPFDs considering the overall physical processes.

Bibliography

[1] Baer, W. et al., “Some aspects of fission counter design”, Review of Scientific Instruments 23 (1) p. 55 (1952)

[2] Baer, W. et al., “A high sensitivity fission counter”, Review of Scientific Instruments 24 (2) p. 138 (1953)

[3] Baer, W. et al., “Fission Counter”, US Patent 2,809,313 (1957)

[4] Bell, et al., “Nuclear reactor theory”, Van Nostrand Reinhold Co., New York (1970)

[5] Biagi, S. F., Nucl. Instr. and Meth. A 421 p. 234 (1999)

[6] Bignan, G. et al., “Sub-miniature fission chamber with tight feedthrough”, PATENT CEA 94-14293 (1994)

[7] Blandin, C. et al., "Development and modeling of neutron detectors for in-core measurement requirements in nuclear reactors," Reactor Dosimetry: Radiation Metrology and Assessment, STP13673S, J. Williams, D. Vehar, F. Ruddy, and D. Gilliam, Ed., ASTM International, West Conshohocken, PA, pp. 803-810 (2001)

[8] Blandin, Ch. et al., “Development of new sub-miniature fission chambers: Modeling and experimental tests”, SMORN-VIII Symposium, Göteborg, Sweden, May 27-31 (2002)

[9] Bridge, M.J. et al., “Concluding experiments in the Windscale AGR”, Nuclear Energy, 21 (1) (1982)

[10] Cabellos, O. et al., “Assessment of fissionable material behavior in fission chambers”, Nucl. Instr. Methods A 618 p. 248–259 (2010)

[11] Cabellos, O. et al., “Propagation of nuclear data uncertainties in transmutation calculations using ACAB code”, International Conference on Nuclear Data for Science and Technology (2010)

[12] Carpenter, D. et al., “TREAT core instrumentation report”, MIT Nuclear Reactor Laboratory (2016)

[13] Chabod, S. P. et al., Nucl. Instr. and Meth. A 566 p. 633 (2006)

[14] Chabod, S. P., "Saturation current of miniaturized fission chambers," Nucl. Instr. and Meth. A, vol. 598, p. 578 (2009)

[15] Chabod, S. et al., "Improvements in the modeling of micro fission chambers operated in current mode," 2009 1st International Conference on Advancements in Nuclear Instrumentation, Measurement Methods and their Applications, Marseille, pp. 1-6 (2009)

[16] DuBridge, R. A., “Campbell theorem - system concepts”, IEEE Trans. Nucl. Sci. NS-14 P. 241 (1967)

[17] Elter, Zs. et al., “Performance investigation of the pulse and Campbelling modes of a fission chamber using a Poisson pulse train simulation code”, Nucl. Instrum. Methods Phys. Res. Sect. A: Accel. Spectrometers, Detect. Assoc. Equip. 774 60–67 (2015)

[18] Forrest, R.A., “The European Activation System: EASY-2007 overview”, UKAEA FUS 533 (2007)

[19] Fadil, M. et al., “Development of fission micro-chambers for nuclear waste incineration studies” Nucl. Instr. And Meth. A476, PP313 (2002)

[20] Filliatre, P. et al., “Reasons why Plutonium-242 is the best fission chamber deposit to monitor the fast component of a high neutron flux”, Nucl. Instrum. and Methods A 593 p. 510 (2008)

[21] Filliatre , P. et al., "Joint estimation of the fast and thermal components of a high neutron flux with a two on-line detector system", Nuclear Instruments And Methods in Physics Research Section A, 603 (3), p. 415-420 (2009)

[22] Filliatre, P. et al., "Monitoring the fast neutrons in a high flux: the case for 242Pu fission chambers," 2009 1st International Conference on Advancements in Nuclear Instrumentation, Measurement Methods and their Applications, Marseille, 2009, pp. 1-4.

[23] Filliatre, P. et al., “A Monte Carlo Simulation of the fission chambers neutron-induced pulse shape using the GARFIELD suite”, Nucl. Instrum. Methods Phys. Res. A, 678, pp. 139–147 (2012)

[24] Geslot, B. et al., "Development and manufacturing of special fission chambers for in-core measurement requirements in nuclear reactors," 2009 1st International Conference on Advancements in Nuclear Instrumentation, Measurement Methods and their Applications, Marseille, pp. 1-4 (2009)

[25] Geslot, B. et al., "Method to calibrate fission chambers in Campbelling mode," 2011 2nd International Conference on Advancements in Nuclear Instrumentation, Measurement Methods and their Applications, Ghent, pp. 1-4 (2011)

[26] Geslot, B. et al., "Impact of Gas Pressure on Fission Chamber Sensitivity in Campbelling Mode," in IEEE Transactions on Nuclear Science, vol. 61, no. 4, pp. 2235-2239 (2014)

[27] Goodings, A, “Present status of high-temperature radiation detectors in the U.K.”, IAEA Panel on Instrumentation for Nuclear Power Control, Vienna (1969)

[28] Goodings, A., “The residual currents obtained from DC (mean current) fission chambers”, AEEW-M—1348, United Kingdom (1975)

[29] Goodings, A. et al., “The wide range in-core neutron measurement system used in the Windscale AGR concluding experiments”, IAEA Specialist Meeting on Gas Cooled Reactor Core High Temperaturef Instrumentation, 15-17 June (1982)

[30] Guéry, M., “Improvements in or Relating to a Miniature Neutron-Fission Ionisation Chamber”, Patent GB 938, 594 (1963)

[31] Hasegawa, K. et al., " A new neutron-flux detection method for fission chamber counting systems," in IEEE Transactions on Nuclear Science, vol. 23, no. 1, pp. 833-838 (1976)

[32] Hermann, O.W. et al., “ORIGEN-S: SCALE system module to calculate fuel depletion, actinide transmutation, fission product buildup and decay, and associated radiation source terms (NUREG/CR--0200-Vol2). United States” (1984)

[33] Jammes, C. et al. “Research activities in fission chamber modeling in support of the nuclear energy industry”, IEEE Transactions on Nuclear Science 57.6 p. 3678-3682 (2010)

[34] Jammes, C. et al., "Assessment of the high temperature fission chamber technology for the French fast reactor program," 2011 2nd International Conference on Advancements in Nuclear Instrumentation, Measurement Methods and their Applications, Ghent, p. 1-9 (2011)

[35] Jammes, C. et al., "On the impact of the fissile coating on the fission chamber signal," Nucl. Instr. and Meth. A, vol. 681, p. 101 (2012)

[36] Keddar, A. et al. , “Neutron Fluence Measurements”, Series No.: 107, Sect. IV.3.3, Technical Report, IAEA (1970)

[37] Knoll, G. F., “Radiation Detection and Measurement”, 2nd Edition, John Wiley & Sons, Inc., New York (1989)

[38] Koch, L.,“Nouveau détecteur de neutrons par fission,” France Patent FR 1.147.321 (1957)

[39] Lemmel, H. D., "JEF-2: Radioactive decay data, an evaluated nuclear data library by the NEA DATA BANK", IAEA-NDS-Documentation series (1994)

[40] Lescop, B. et al., "Marine: a fast fully digitalized wide range neutron monitor system," 2000 IEEE Nuclear Science Symposium. Conference Record (Cat. No.00CH37149), Lyon, pp. 5/86-5/90 vol.1 (2000)

[41] Lescop, B. et al., "A new system for in-core wide range neutron monitoring," IEEE Symposium Conference Record Nuclear Science 2004., Rome, pp. 1567-1570 Vol. 3 (2004)

[42] Letourneau, A. et al., "Recent developments on micrometric fission chambers for high neutron fluxes," 2009 1st International Conference on Advancements in Nuclear Instrumentation, Measurement Methods and their Applications, Marseille, pp. 1-8 (2009)

[43] Lux, I. et al., “Higher order Campbell techniques for neutron flux measurement”, Nucl. Instr. Meth., V202, 469-475 (1983)

[44] McGregor, D.S. et al., “Micro-Pocket Fission Detectors (MPFD) for in-core neutron flux monitoring”, Nucl. Instrum. Meth. A554, 494–499 (2005)

[45] McGregor, D. S., “Principles of Radiation Detection and Measurement Lecture Notes”, Mechanical and Nuclear Engineering Dept., Kansas State University, unpublished, Spring (2016)

[46] Normand, S. et al., “A new small fission chamber for in core and wide range neutron flux measurement”, IMORN-29 Budapest (2004)

[47] Ohmes, M.F. et al., “Development of Micro-Pocket Fission Detectors (MPFD) for near-core and in-core neutron flux monitoring”, in: SPIE Proc. Hard X-Ray and Gamma-Ray Detector Physics, vol. 5198, pp. 234–242 (2004)

[48] Ohmes, M.F. et al., “Micro-pocket fission detector (MPFD) performance characteristics”, in: Conf. Proc. IEEE Nucl. Sci. Symp., San Diego CA, USA, Oct. 29–Nov. 4 (2006)

[49] Oriol, L. et al., “In-pile CFUZ53 Sub-miniature fission chambers qualification in BR2 under PWR condition”, Proc. Joint TRTR-IGORR Meeting, Gaithersburg, MD, USA, Sept. 12-16 (2005)

[50] Palestini, S. et al.,“Space Charge in Ionization Detectors,” LARTPC-doc 528 6 (2010)

[51] Patel, V. K. et al., “MCNP6 simulated performance of Micro-Pocket Fission Detectors (MPFDs) in the Transient REActor Test (TREAT) facility”, Annals of Nuclear Energy, v. 104, p. 191-196 (2017)

[52] Pontes, E. W. et al., "Using cumulants and spectra to model nuclear radiation detectors," in IEEE Transactions on Nuclear Science, vol. 53, no. 3, pp. 1292-1298 (2006)

[53] Popper, “LMFBR neutron monitoring systems—A review of the state-of-the-art,” IEEE Trans. Nucl. Sci, vol. NS-21, no. 1, pp. 741–749, Feb. 1974.

[54] Poujade, O. et al., “Modeling of the saturation current of a fission chamber taking into account the distortion of electric field due to space charge effects”, Nucl. Instr. and Meth. A 433 p. 673 (1999)

[55] Reichenberger, M. A. et al. , "First-order numerical optimization of fission-chamber coatings using natural uranium and thorium," IEEE Nuclear Science Symposium and Medical Imaging Conference (NSS/MIC), Seattle, WA, 2014, pp. 1-4 (2014)

[56] Reichenberger, M. A. et al. , "Micro-Pocket Fission Detectors (MPFDs) for in-core neutron detection," Annals of Nuclear Energy, no. 87, pp. 318-323 (2016)

[57] Rossi, B. et al., “Ionization Chambers and Counters”, McGraw-Hill Book Company, Inc., New York (1949)

[58] Sanz, J. et al., “ACAB-2008, Activation Abacus Code V2008, NEA Data Bank (NEA-1839) (2009)

[59] Sublet, J. C. et al., “The European Activation File:EAF-97 Report File", Rev. 1., UKAEA/Euratom Fusion Association.

[60] Shultis, J. K., “An MCNP Primer”, Kansas State University, Department of Mechanical and Nuclear Engineering (2011)

[61] Trama, J.-C. et al., " Advanced digital signal processing technique for neutron flux Measurement in a nuclear power plant" IEEE NSS 2000, Lyon15-20 October (2000)

[62] Trama, J.C. et al., “Marine : A New Wide Range Neutron Monitoring System Concept”, ICONE 9, Nice (2001)

[63] Trapp, J. et al., “High tempera-ture fission chambers: State-of-the-art,” in Proc. Specialists’ Meeting, In-Core Instrumentation and Core Assessment, Mito-shi, Japan (1996)

[64] Tsilanizara, A. et al., “DARWIN: an evolution code system for a large range of applications”, Journal of Nuclear Science and Technology, 37:sup1, 845-849 (2000)

[65] Tsoulfanidis, N. , “Measurement and Detection of Radiation”, 4th Edition, CRC Press, Taylor & Francis Group, New York (2015)

[66] Unruh, T. et al., “NEET Micro-Pocket Fission Detector – FY 2013 Status Report”, Idaho National Laboratory (INL), Idaho Falls (2013)

[67] Veenhof, R., “GARFIELD, a drift chamber simulation program, CERN, 1994, CERN program library,” Nucl. Instr. and Meth. A, vol. 419, p. 726 (1998) entry W5050. [Online]. Available: http://cern.ch/garfield

[68] Vermeeren, L. et al.,” In-pile sub-miniature fission chambers testing in BR2”, Proc. 11th Int. Symp. on Reactor Dosimetry, Brussels, Aug. 18-23, 2002, eds. J. Wagemans et al., World Scientific, pp.364-371 (2003)

[69] Vermeeren, L. et al., "Experimental verification of the fission chamber gamma signal suppression by the Campbelling mode," 2009 1st International Conference on Advancements in Nuclear Instrumentation, Measurement Methods and their Applications, Marseille, pp. 1-8 (2009)

[70] Ziegler, J.F. et al., “SRIM - The stopping and range of ions in matter”, Nucl. Instrum. Meth. B 268, 1818–1823 (2010)

[71] http://bwrcs.eecs.berkeley.edu/Classes/IcBook/SPICE/

[72] http://cyclo.mit.edu/drift/www/aboutMagboltz.html

[73] http://root.cern.ch/

[74] https://www.oecd-nea.org/dbdata/data/nds_eval_libs.htm

[75] https://rsicc.ornl.gov/codes/ccc/ccc8/ccc-834.html

[76] http://www.oecd-nea.org/tools/abstract/detail/ccc-0371

[77] https://home.wlu.edu/~levys/kalman_tutorial/